Supplementary Information

Stimulus-activated Ribonuclease Targeting Chimeras for Tumour Microenvironment Activated Cancer Therapy

Yuqi Zhang[1], Jinfeng Zhu[2], Ling Qiu[3], Zhengzhong Lv[1], Zhongsheng Zhao[1], Xingxiang Ren[1], Yirui Guo[1], Yan Chen[1], Miao Li[1], Yurong Fan[4], Zhixin Han[1], Yiming Feng[1], Haibin Shi[1*]

[1]State Key Laboratory of Radiation Medicine and Protection, School of Radiation Medicine and Protection, and Collaborative Innovation Center of Radiological Medicine of Jiangsu Higher Education Institutions, Soochow University, Suzhou 215123, P. R. China. [2]Department of Experimental Medicine, TOR, University of Rome Tor Vergata, Roma 00133, Italy. [3]Key Laboratory of Nuclear Medicine, Ministry of Health, Jiangsu Key Laboratory of Molecular Nuclear Medicine, Jiangsu Institute of Nuclear Medicine, Wuxi 214063, P. R. China. [4]Department of Radiology, The Second Affiliated Hospital of Soochow University, Suzhou 215004, P. R. China.

*e-mail: hbshi@suda.edu.cn

Content

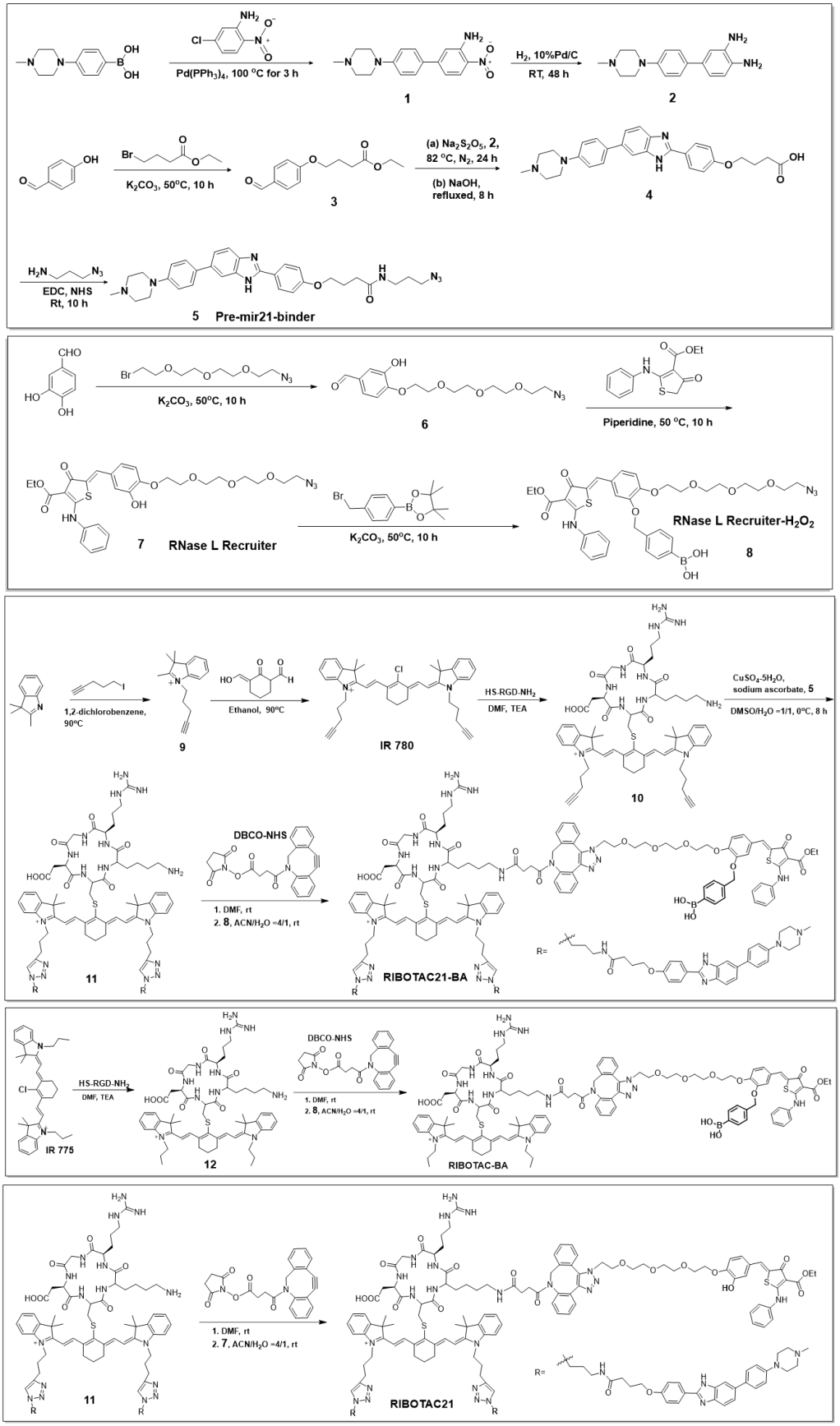

Supplementary Figure. 1. Synthetic route for probe RIBOTAC21-BA and control probe RIBOTAC-BA and RIBOTAC21.

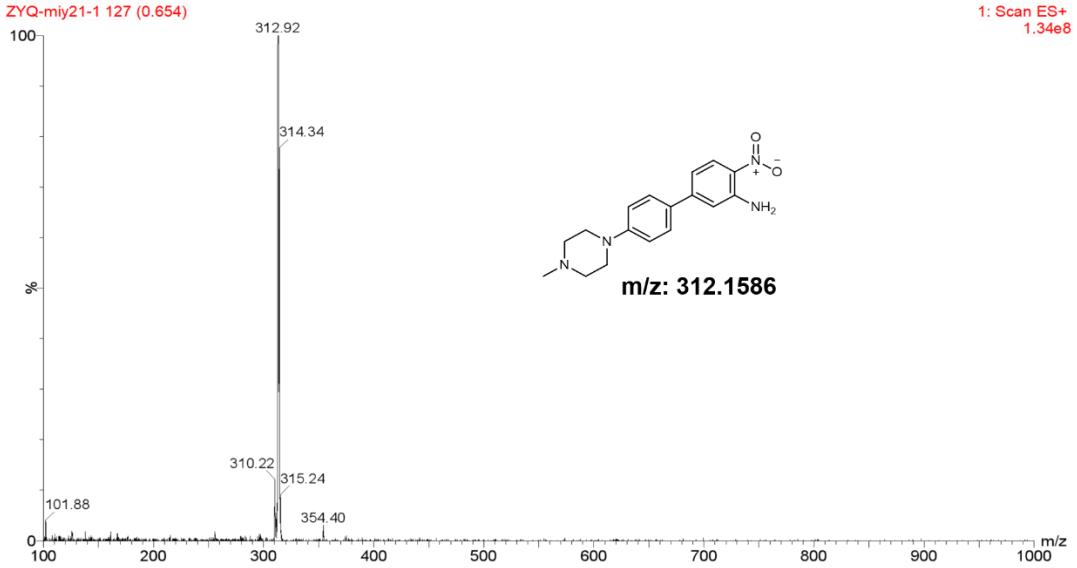

Supplementary Figure. 2. LC-MS spectrum of compound **1**.

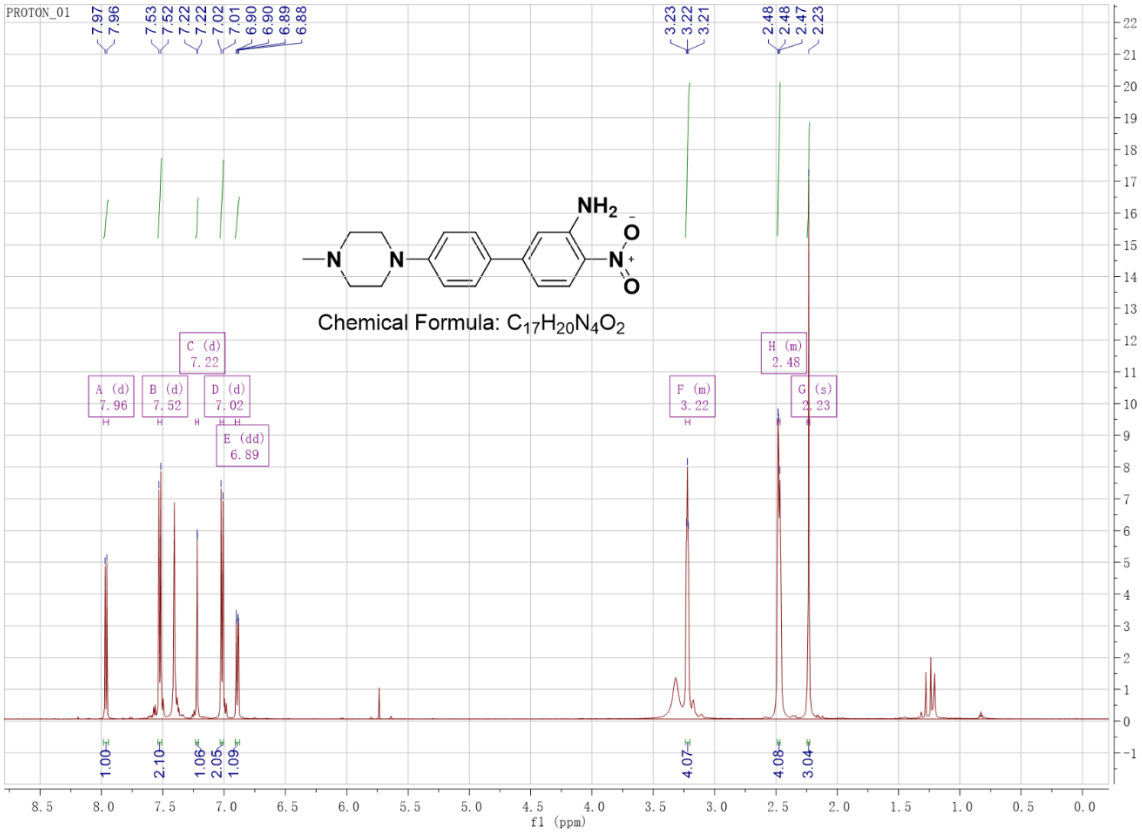

Supplementary Figure. 3. ^{1}H-NMR spectrum of compound **1** (DMSO-*d6*).

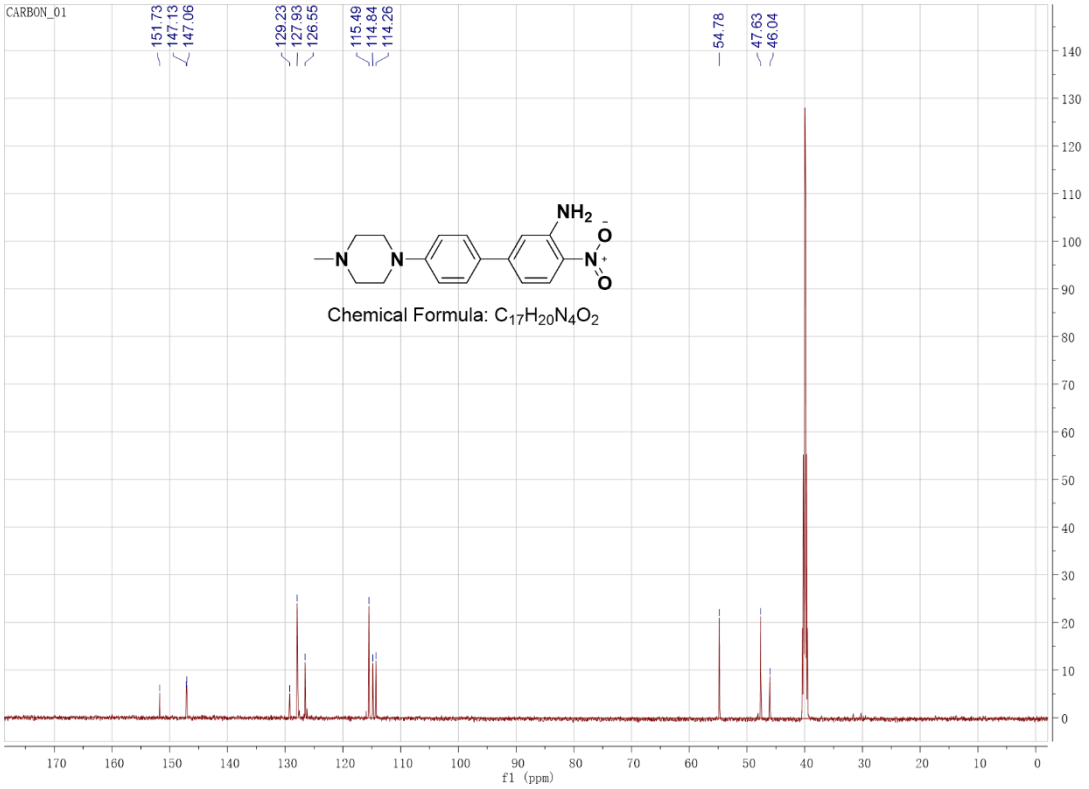

Supplementary Figure. 4. ^{13}C-NMR spectrum of compound **1** (DMSO-*d6*).

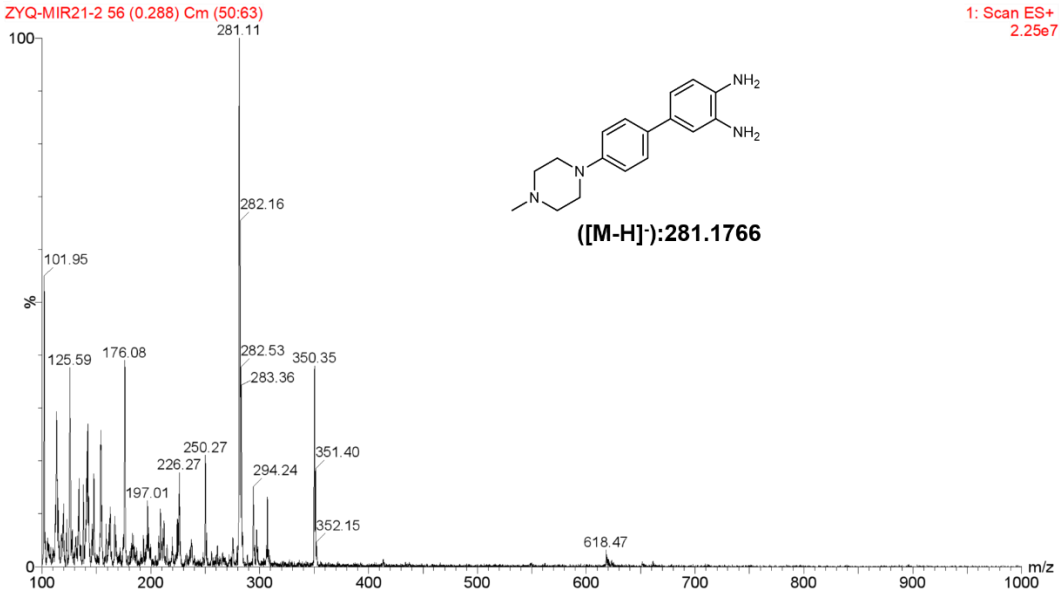

Supplementary Figure. 5. LC-MS spectrum of compound **2**.

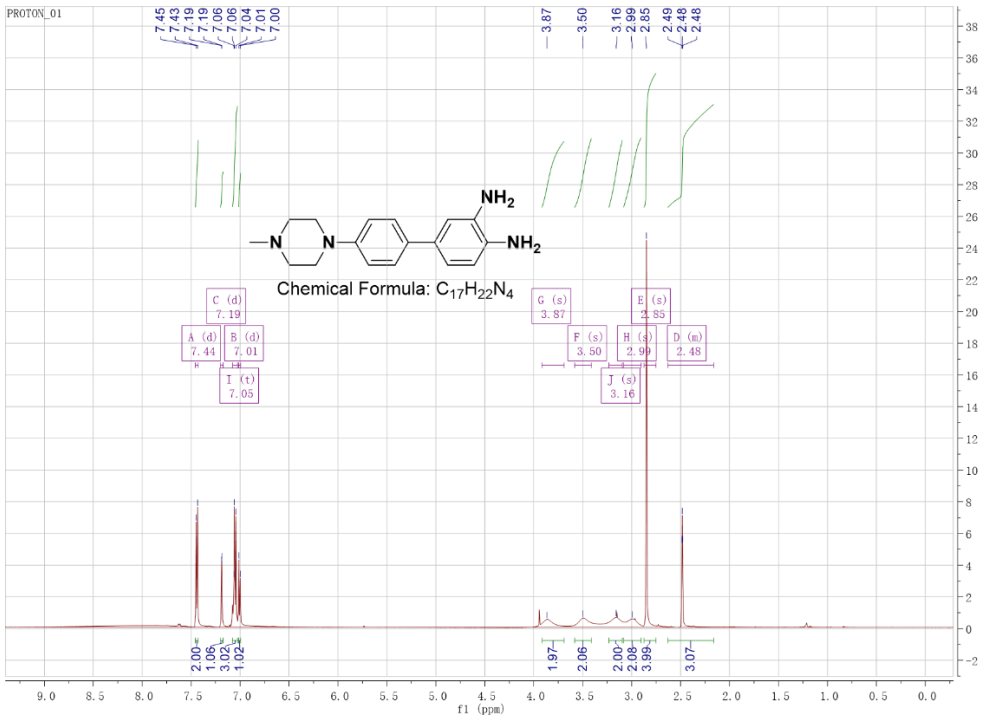

Supplementary Figure. 6. ^{1}H-NMR spectrum of compound **2** (DMSO-*d6*).

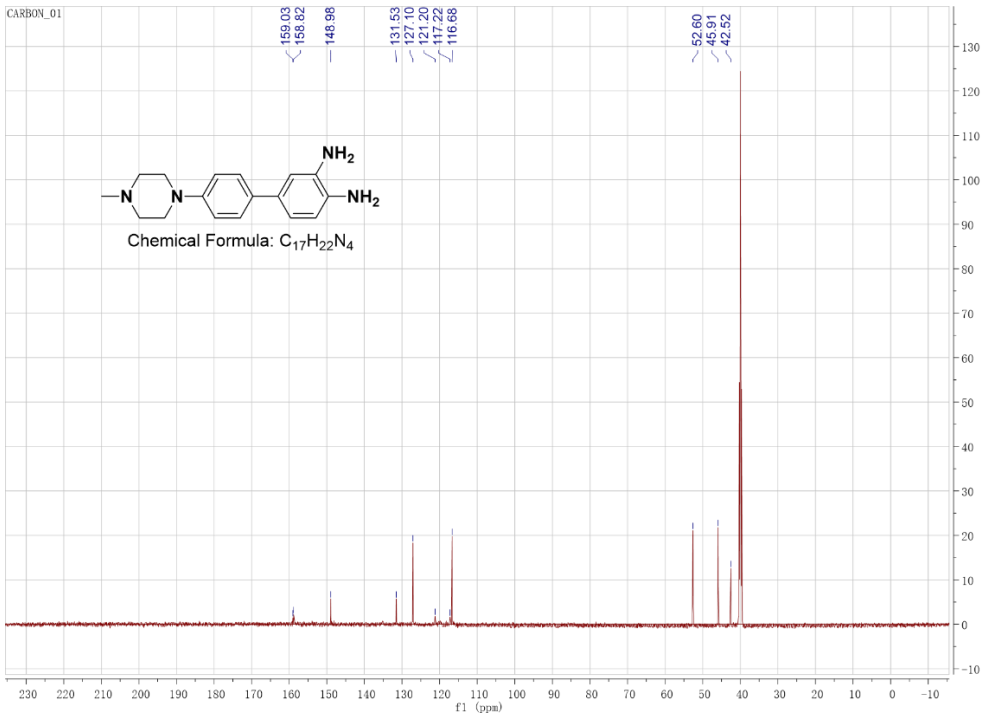

Supplementary Figure. 7. ^{13}C-NMR spectrum of compound **2** (DMSO-*d6*).

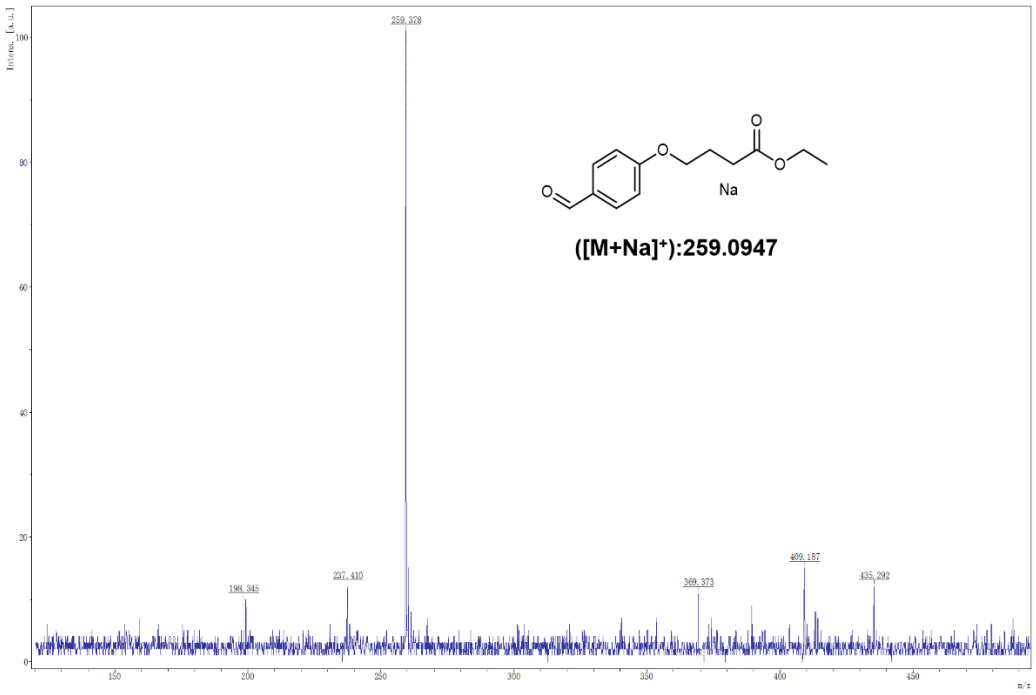

Supplementary Figure. 8. HR-MS spectrum of compound **3**.

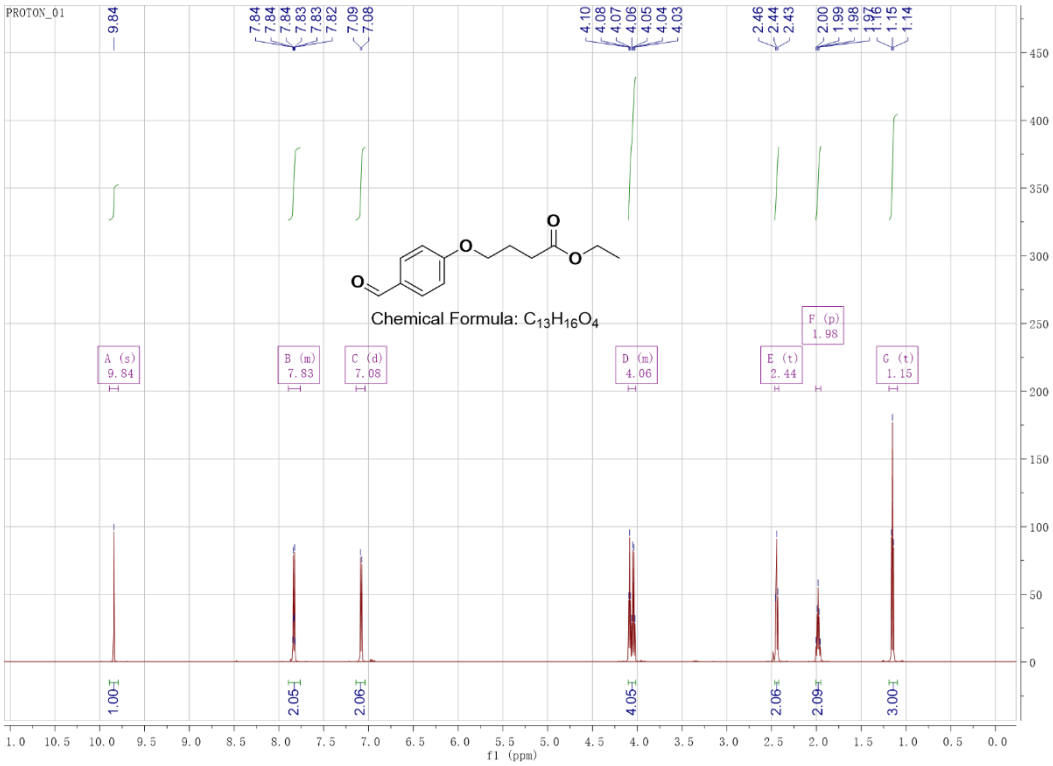

Supplementary Figure. 9. ^{1}H-NMR spectrum of compound **3** (DMSO-*d6*).

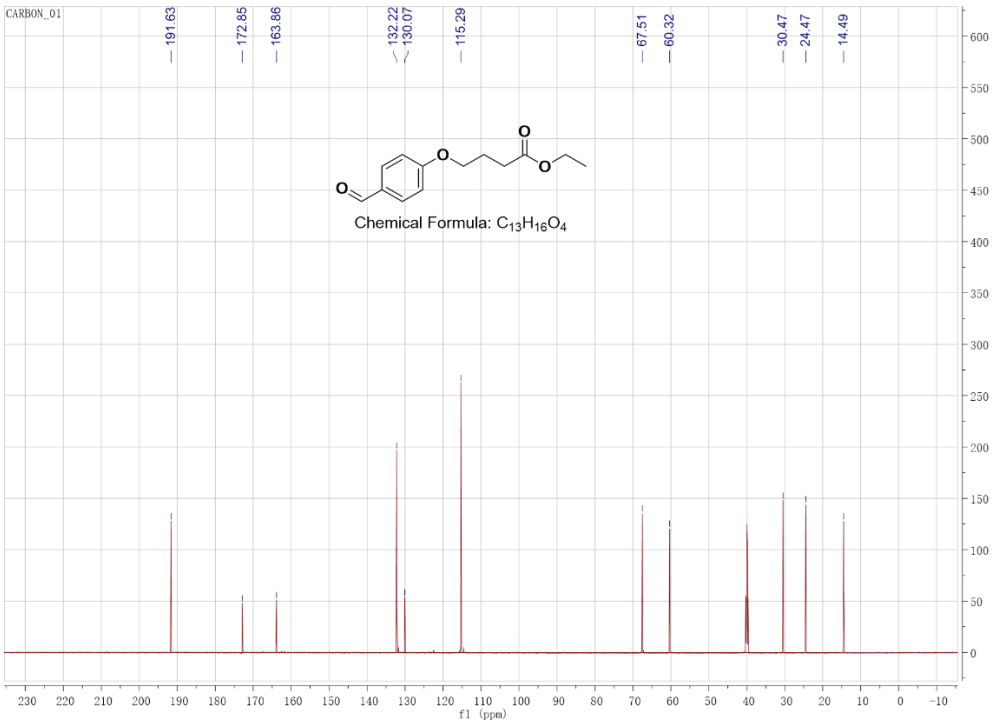

Supplementary Figure. 10. ^{13}C-NMR spectrum of compound **3** (DMSO-*d6*).

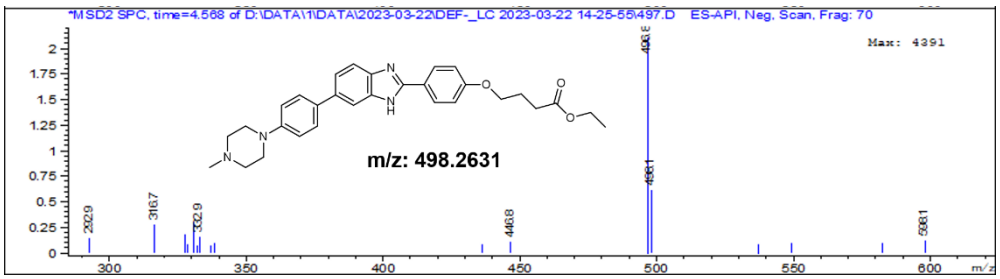

Supplementary Figure. 11. LC-MS spectrum of compound **4-*pre***.

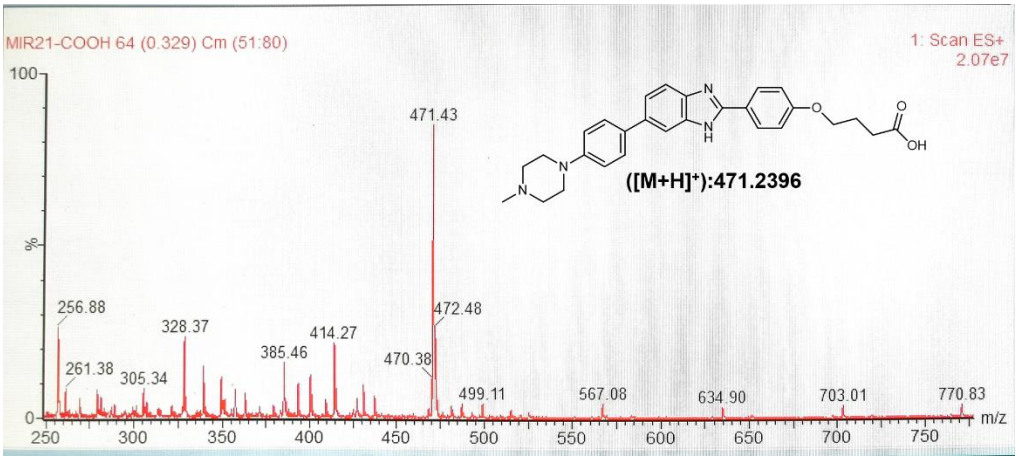

Supplementary Figure. 12. LC-MS spectrum of compound **4**.

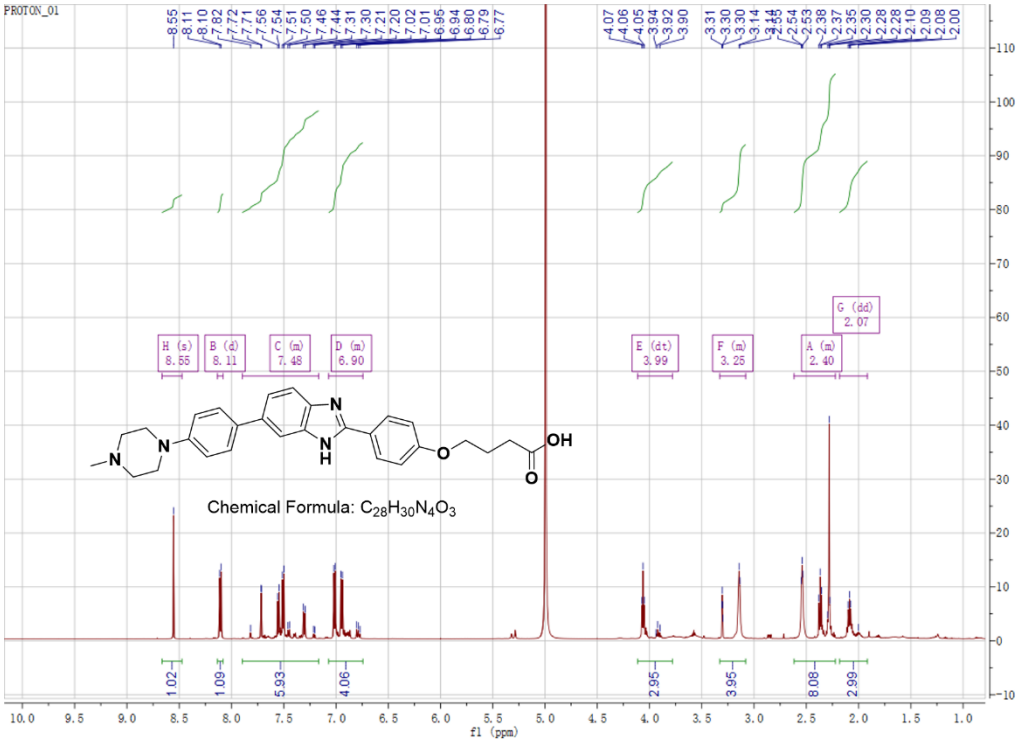

Supplementary Figure. 13. ^{1}H-NMR spectrum of compound **4** (CD_3OD).

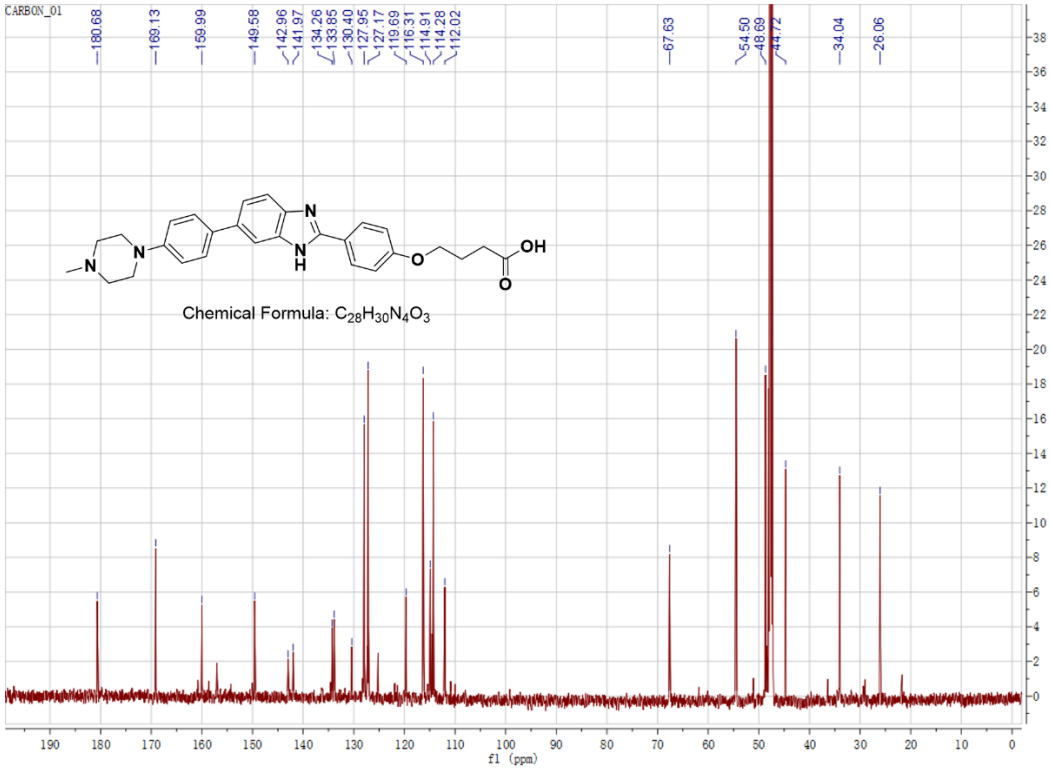

Supplementary Figure. 14. ^{13}C-NMR spectrum of compound **4** (CD_3OD).

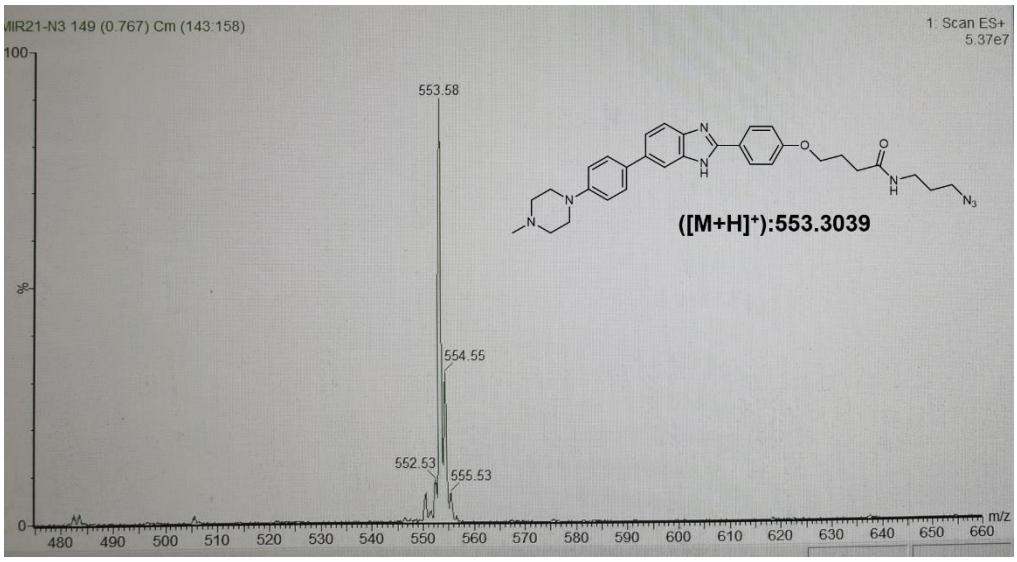

Supplementary Figure. 15. LC-MS spectrum of compound **5**.

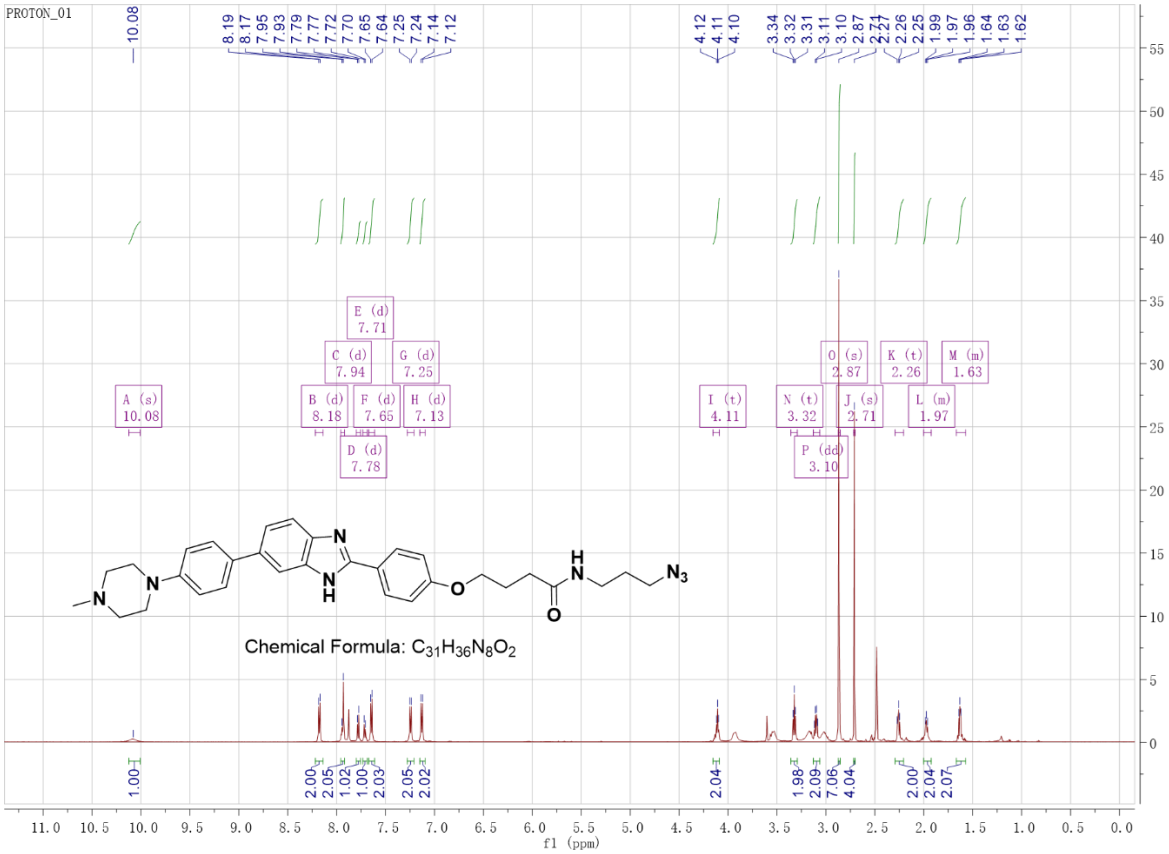

Supplementary Figure. 16. ^{1}H-NMR spectrum of compound **5** (DMSO-*d6*).

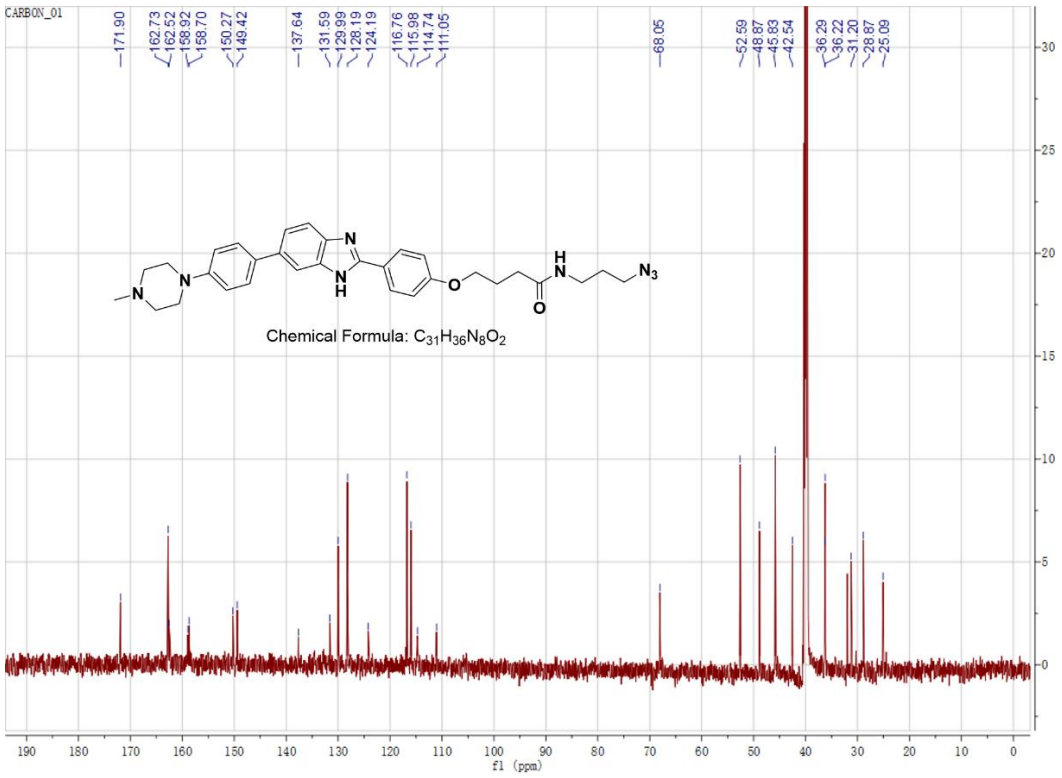

Supplementary Figure. 17. ^{13}C-NMR spectrum of compound **5** (DMSO-*d6*).

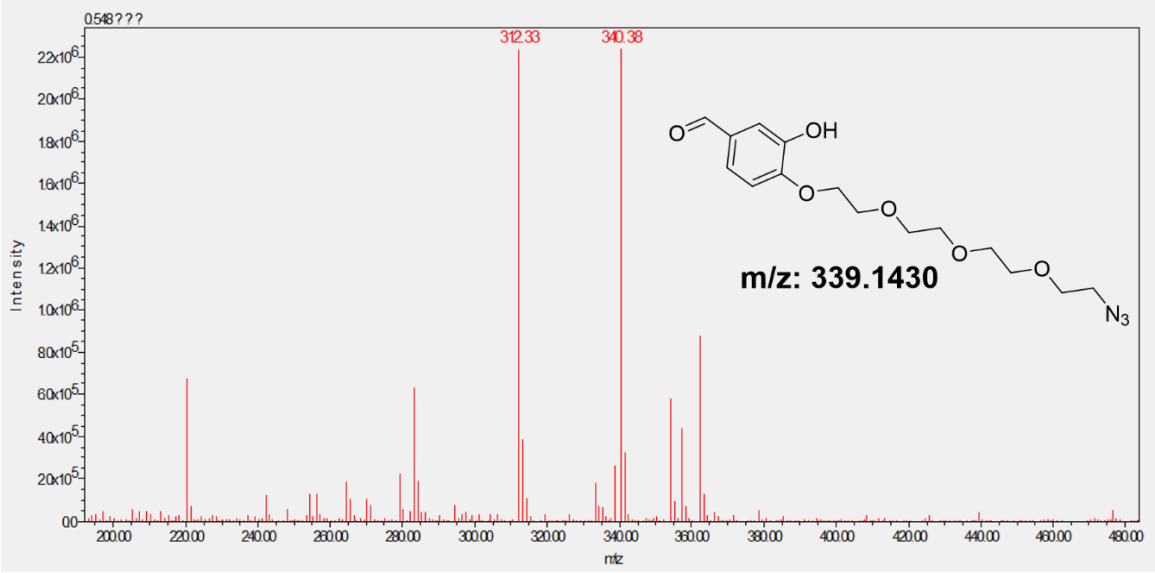

Supplementary Figure. 18. LC-MS spectrum of compound **6**.

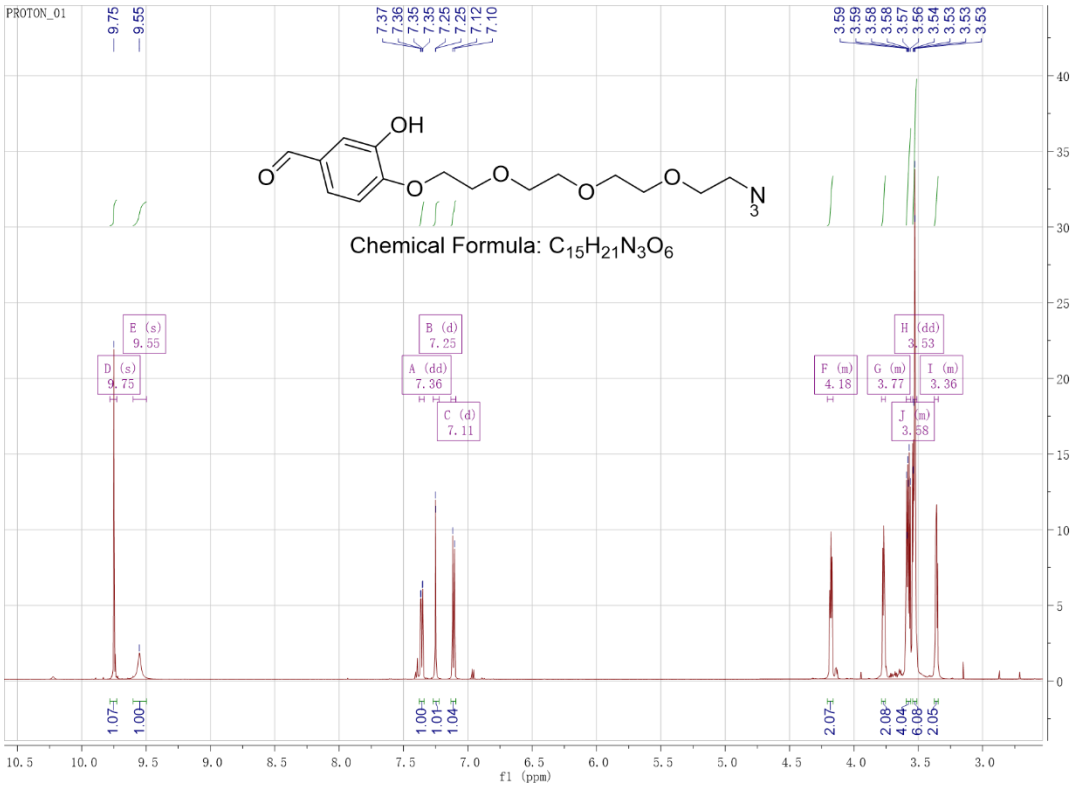

Supplementary Figure. 19. ^{1}H-NMR spectrum of compound **6** (DMSO-*d6*).

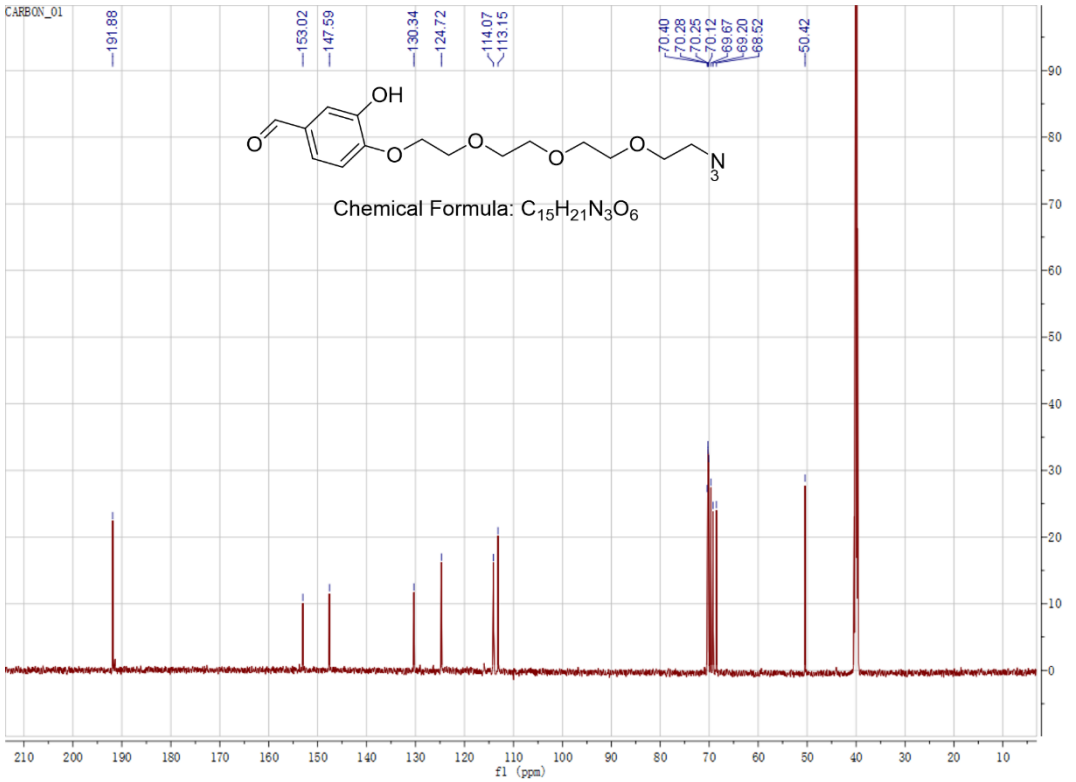

Supplementary Figure. 20. ^{13}C-NMR spectrum of compound **6** (DMSO-*d6*).

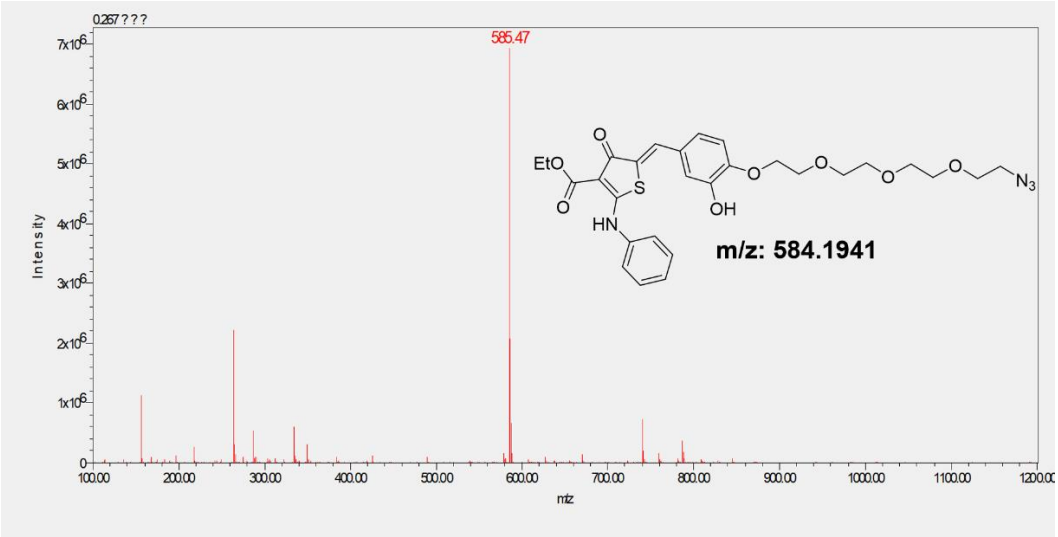

Supplementary Figure. 21. LC-MS spectrum of compound **7**.

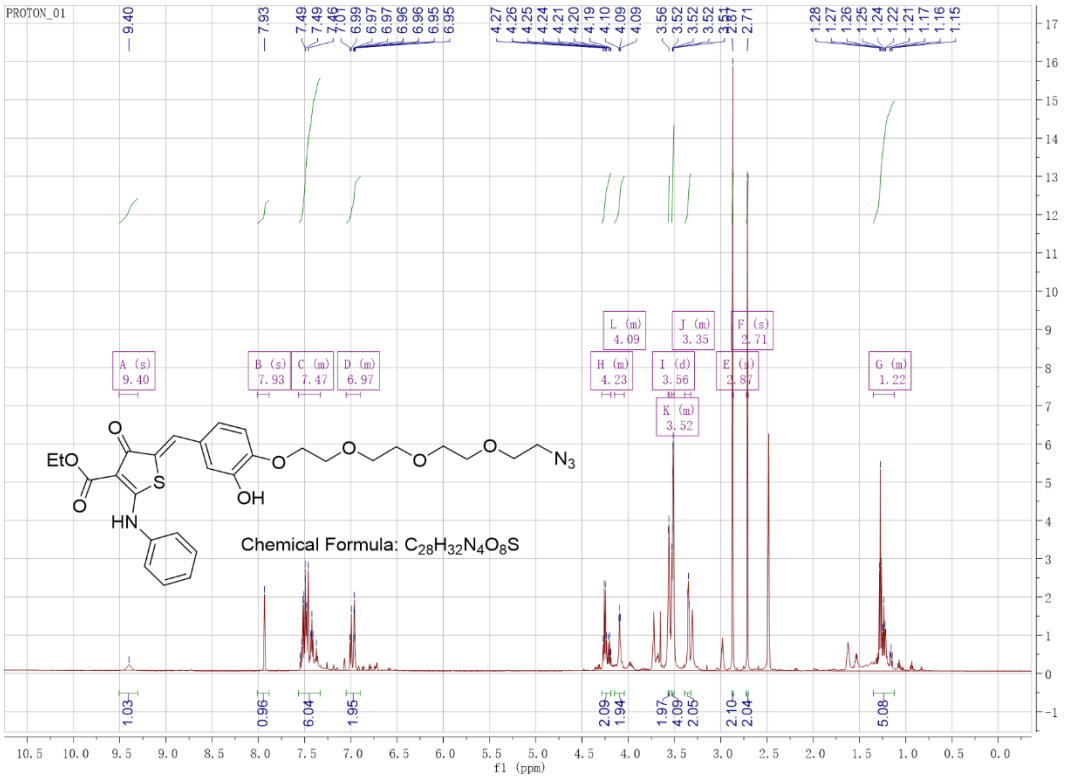

Supplementary Figure. 22. ^{1}H-NMR spectrum of compound **7** (DMSO-*d6*).

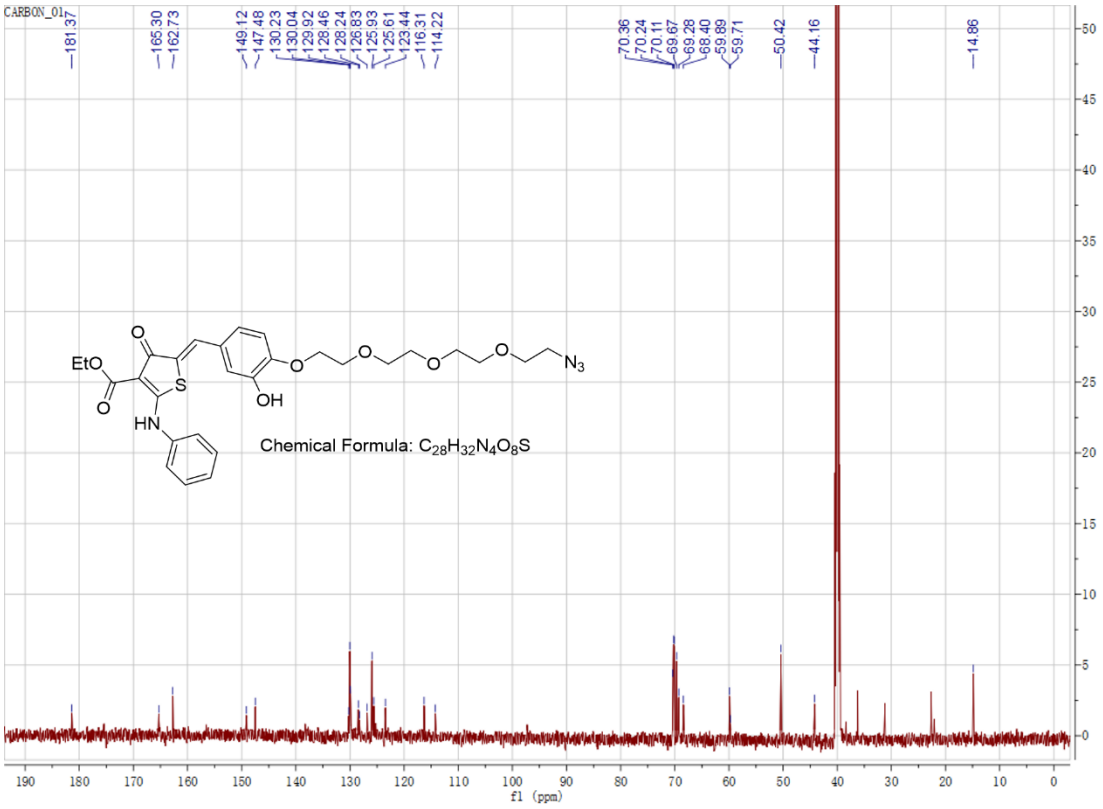

Supplementary Figure. 23. ^{13}C-NMR spectrum of compound **7** (DMSO-*d6*).

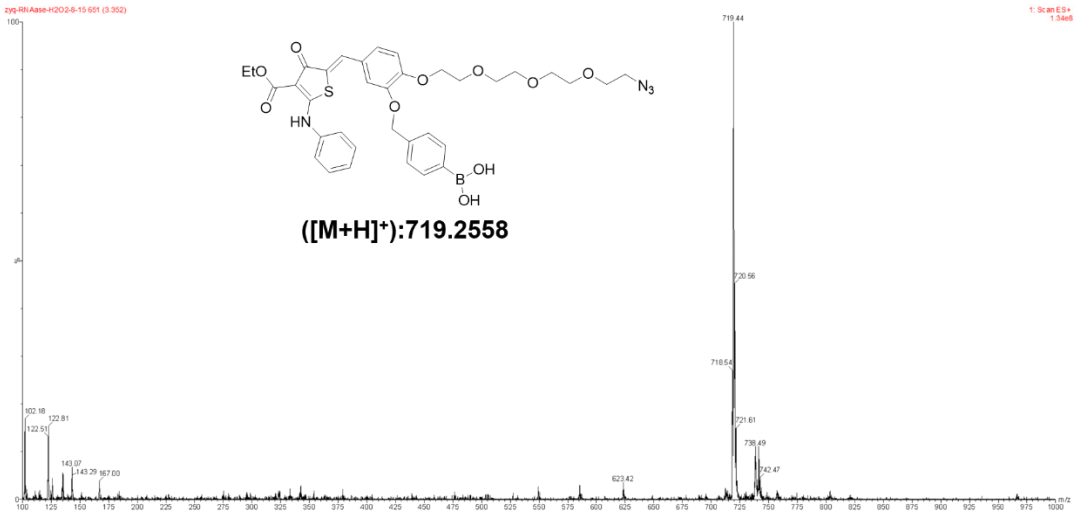

Supplementary Figure. 24. LC-MS spectrum of compound **8**.

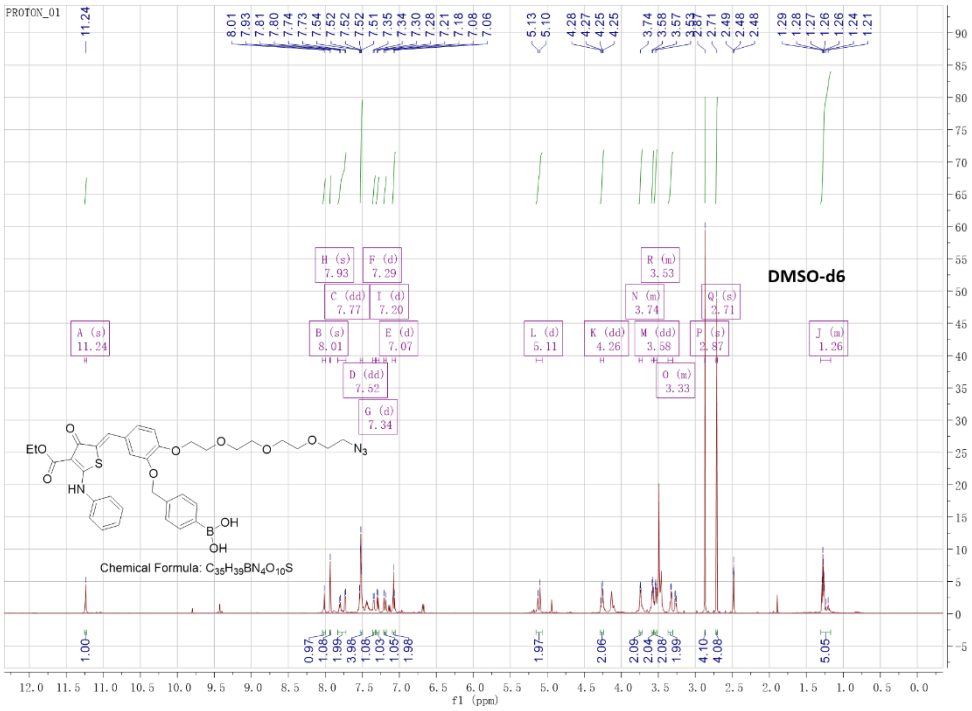

Supplementary Figure. 25. ^{1}H-NMR spectrum of compound **8** (DMSO-*d6*).

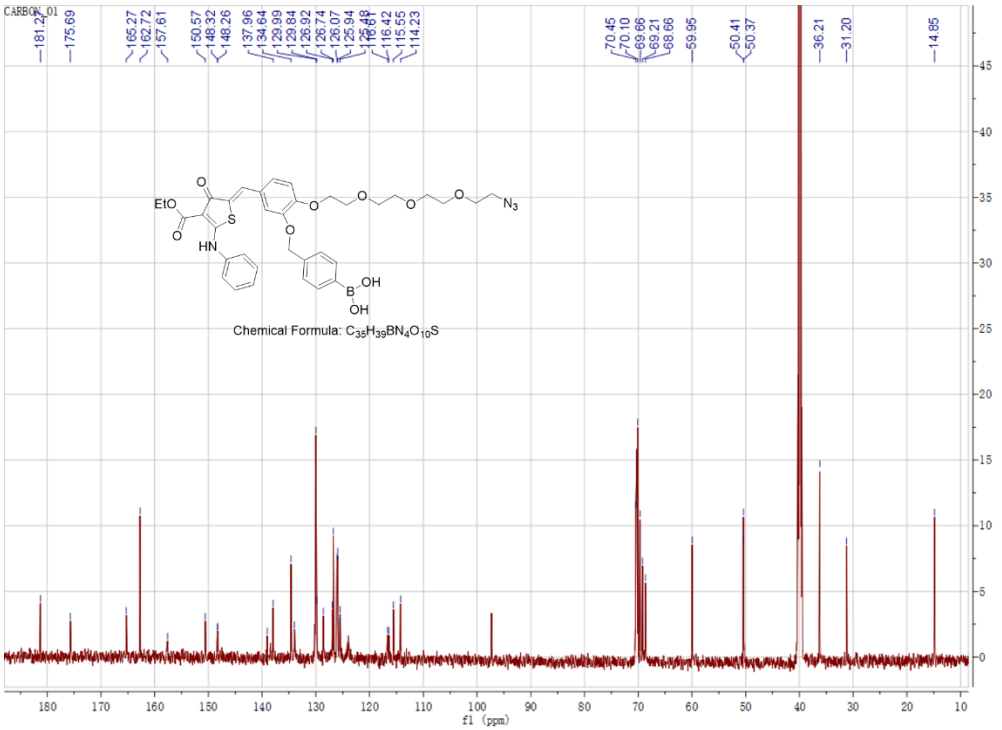

Supplementary Figure. 26. ^{13}C-NMR spectrum of compound **8** (DMSO-*d6*).

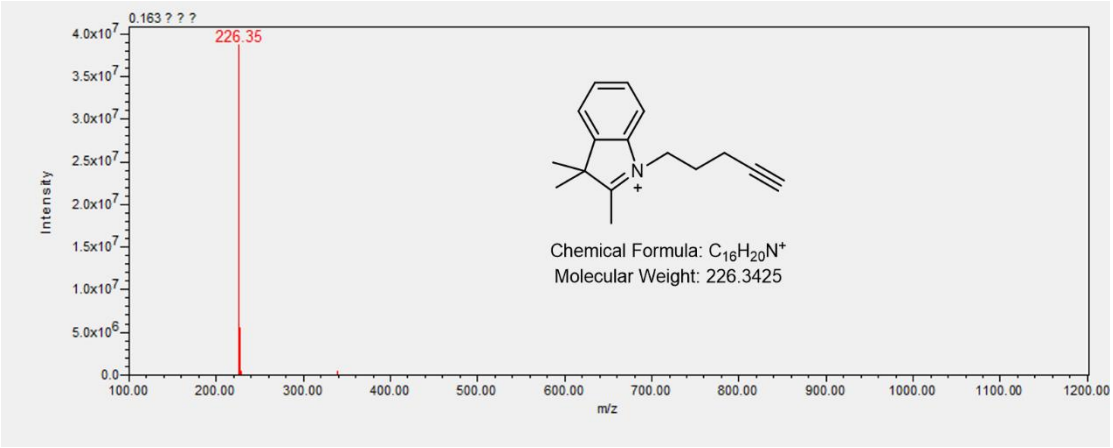

Supplementary Figure. 27. LC-MS spectrum of compound **9**.

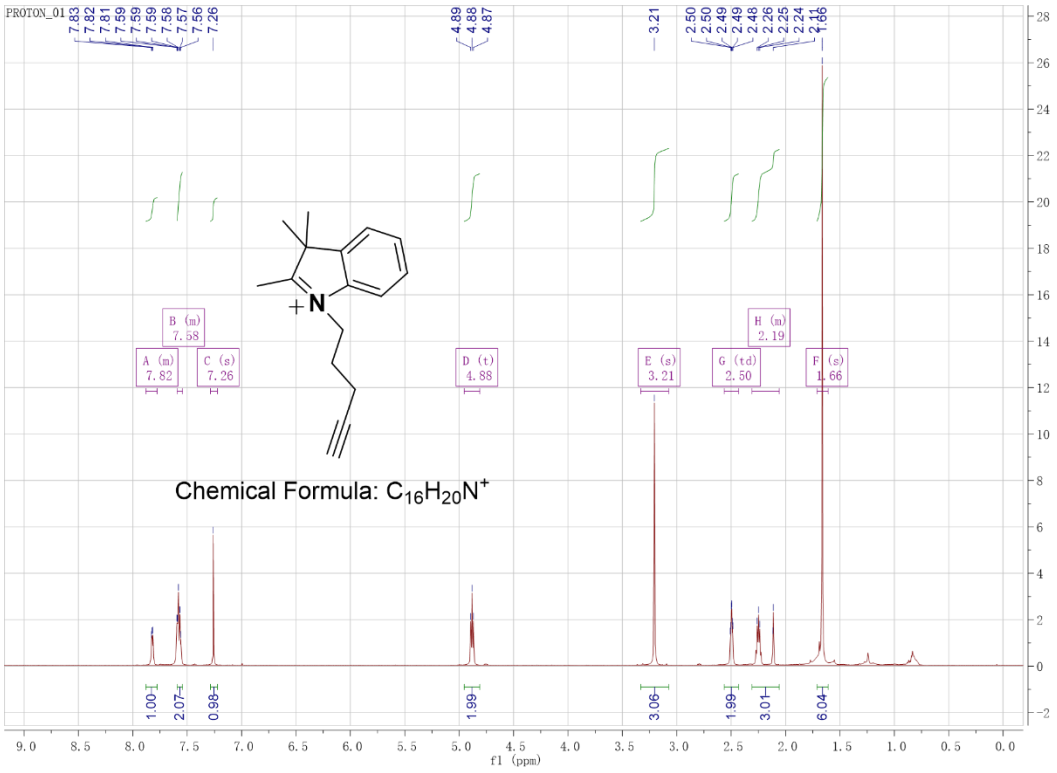

Supplementary Figure. 28. ^{1}H-NMR spectrum of compound **9** (CD_3Cl).

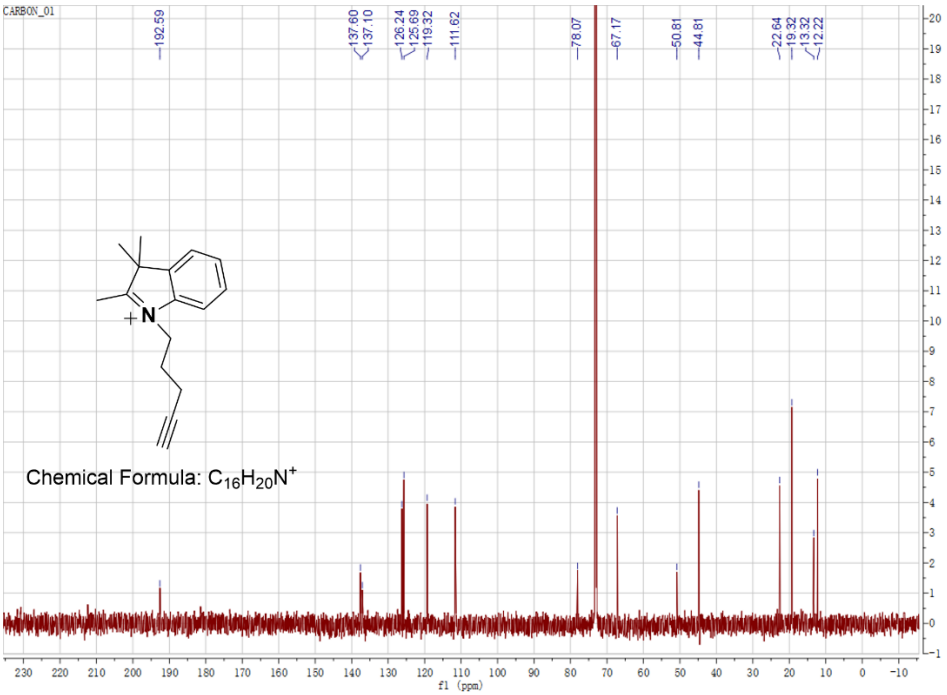

Supplementary Figure. 29. ^{13}C-NMR spectrum of compound **9** (CD_3Cl).

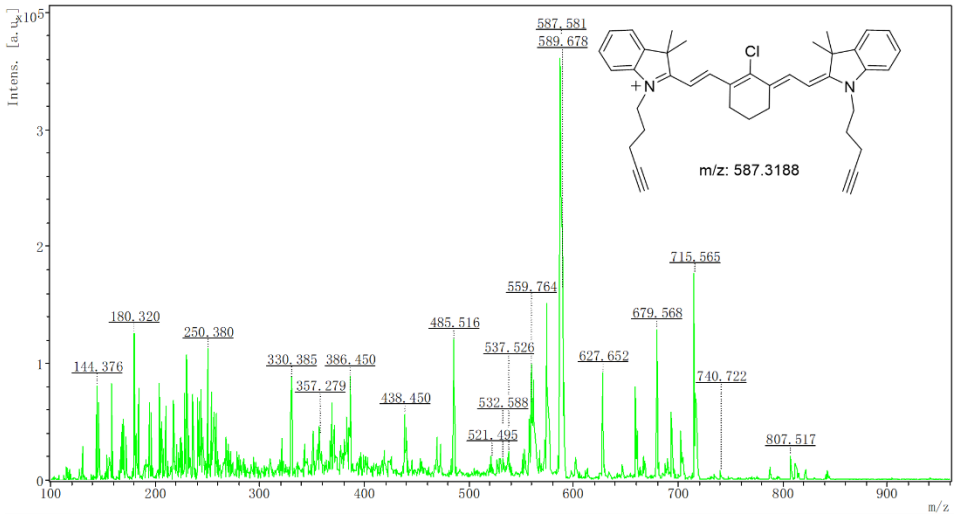

Supplementary Figure. 30. HR-MS spectrum of **IR 780**.

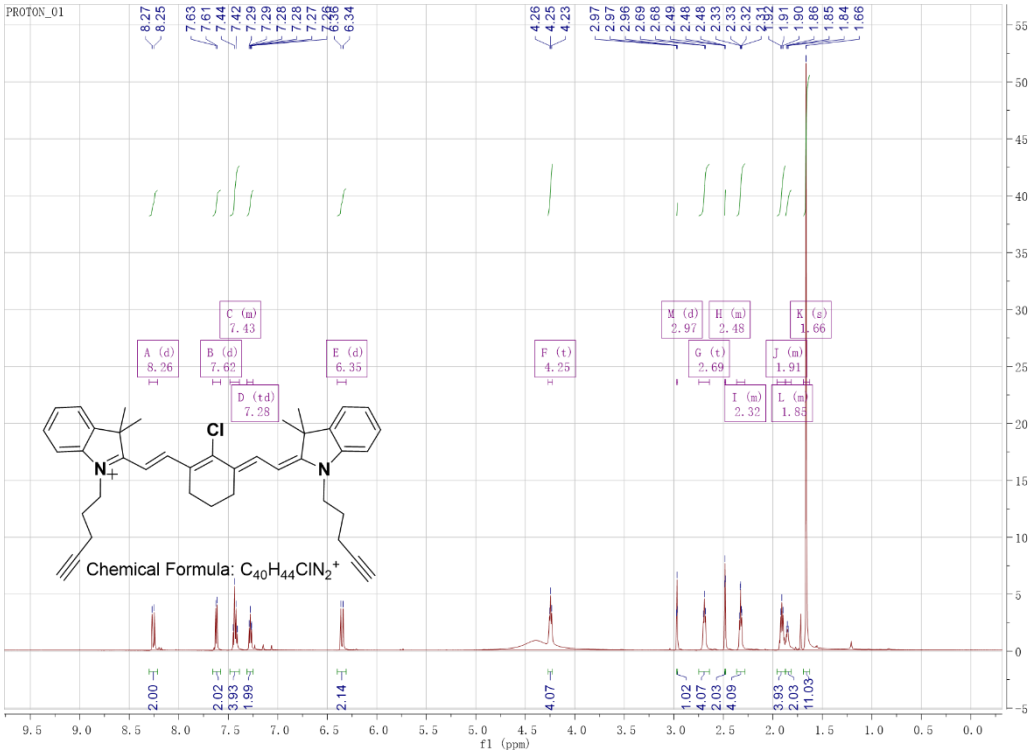

Supplementary Figure. 31. ^{1}H-NMR spectrum of compound **IR 780** (DMSO-*d6*).

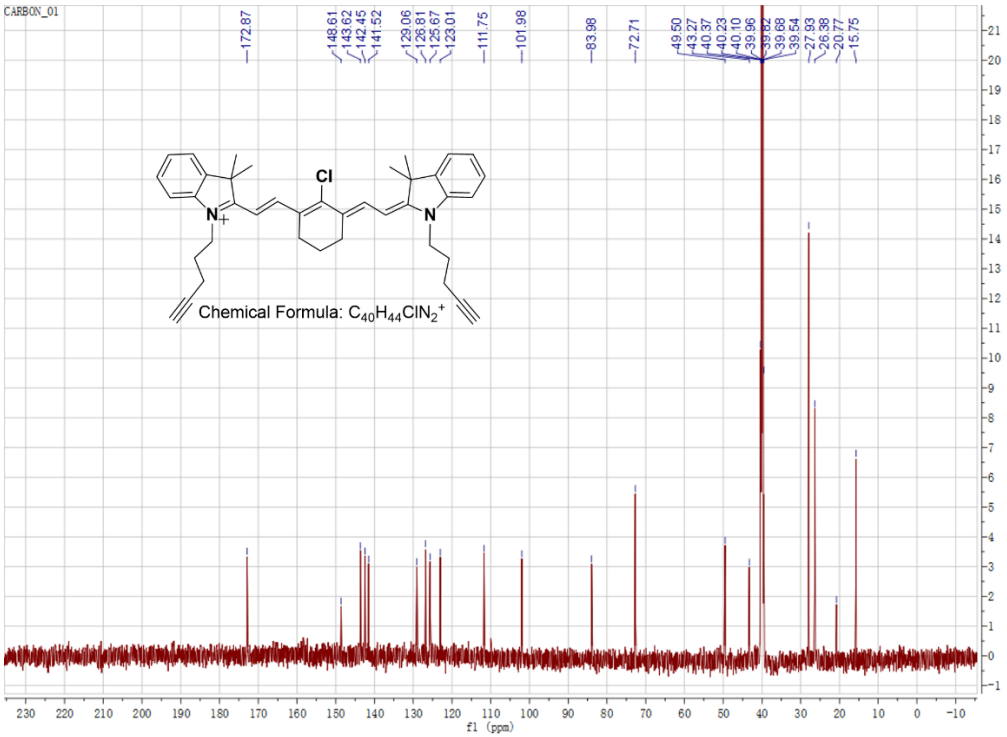

Supplementary Figure. 32. ^{13}C-NMR spectrum of compound **IR 780** (DMSO-*d6*).

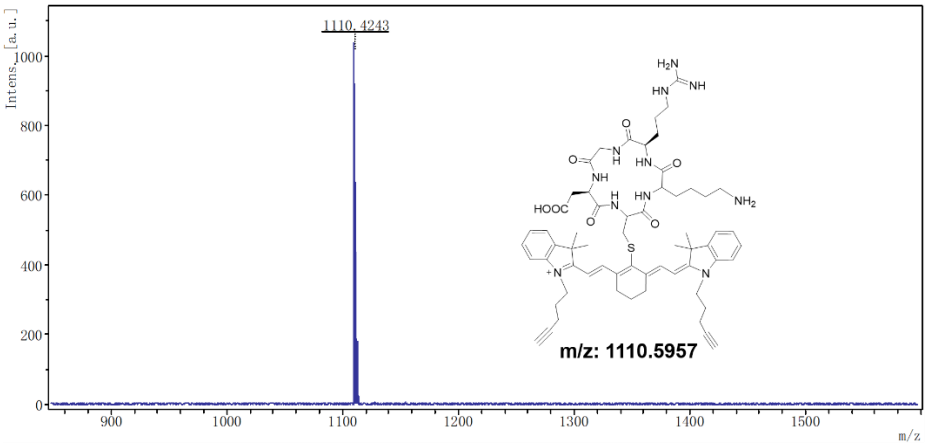

Supplementary Figure. 33. HR-MS spectrum of compound **10**.

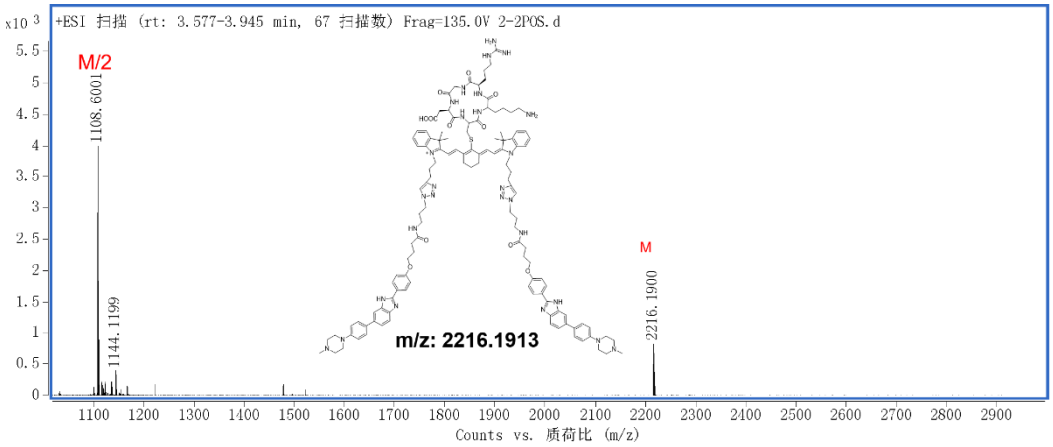

Supplementary Figure. 34. HR-MS spectrum of compound **11**.

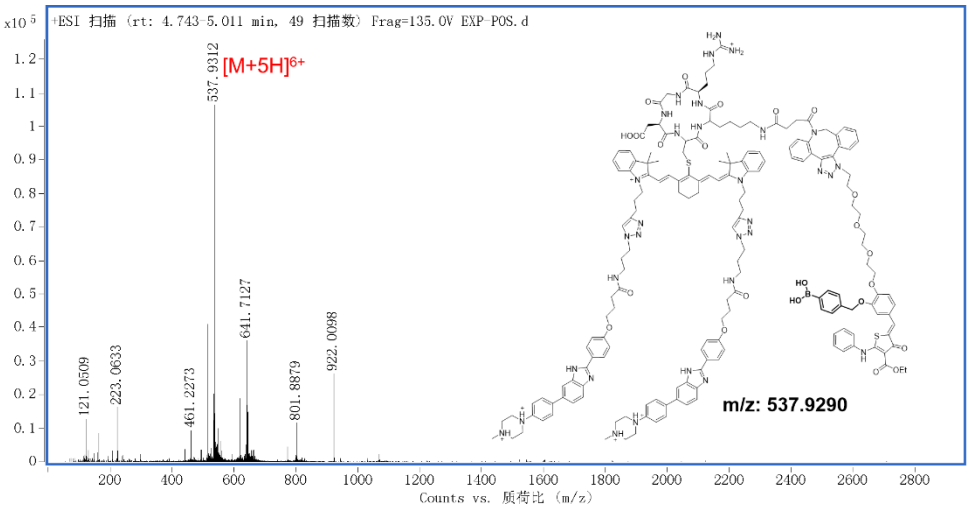

Supplementary Figure. 35. HR-MS spectrum of **RIBOTAC21-BA**.

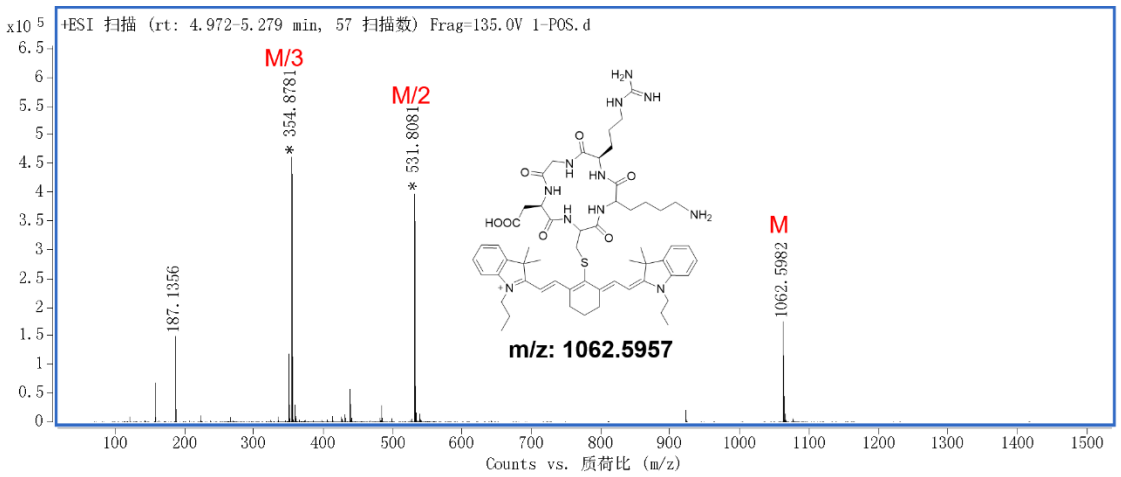

Supplementary Figure. 36. HR-MS spectrum of compound **12**.

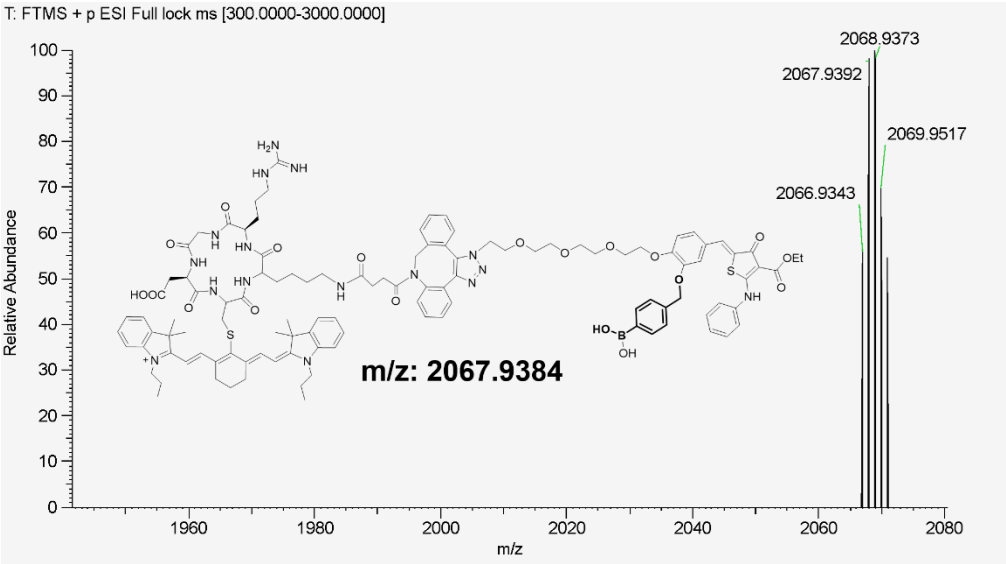

Supplementary Figure. 37. HR-MS spectrum of **RIBOTAC-BA**.

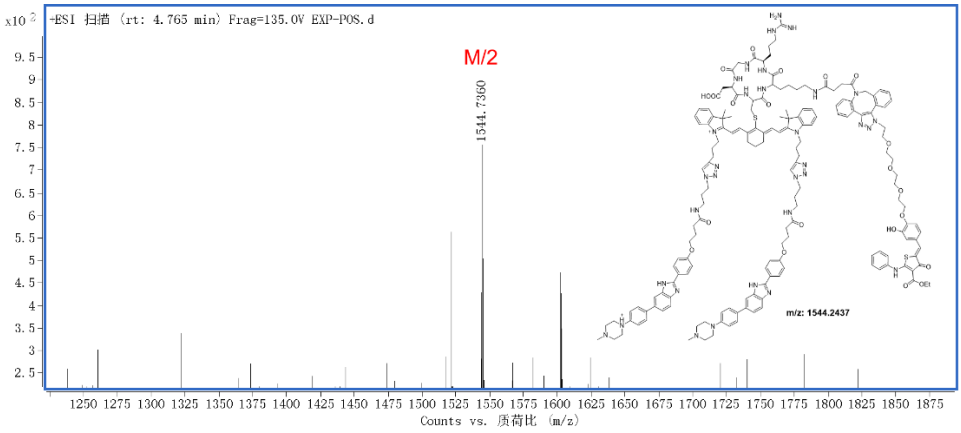

Supplementary Figure. 38. HR-MS spectrum of **RIBOTAC21**.

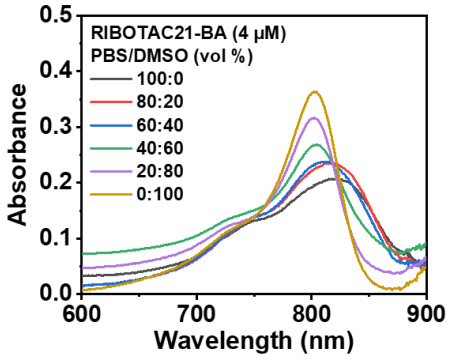

Supplementary Figure. 39. Absorption of RIBOTAC21-BA (5 μM) in different proportions of H_2O_2 and DMSO. Source data are provided as a Source Data file.

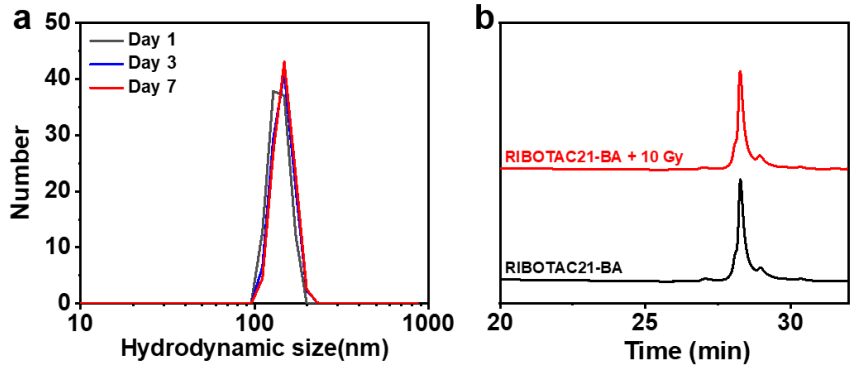

Supplementary Figure. 40. (a) The hydrodynamic size of RIBOTAC21-BA nanoparticles in PBS buffer (pH=7.4) over 7 days. (b) HPLC profiling of RIBOTAC21-BA before and after irradiation of 10 Gy X-ray. Source data are provided as a Source Data file.

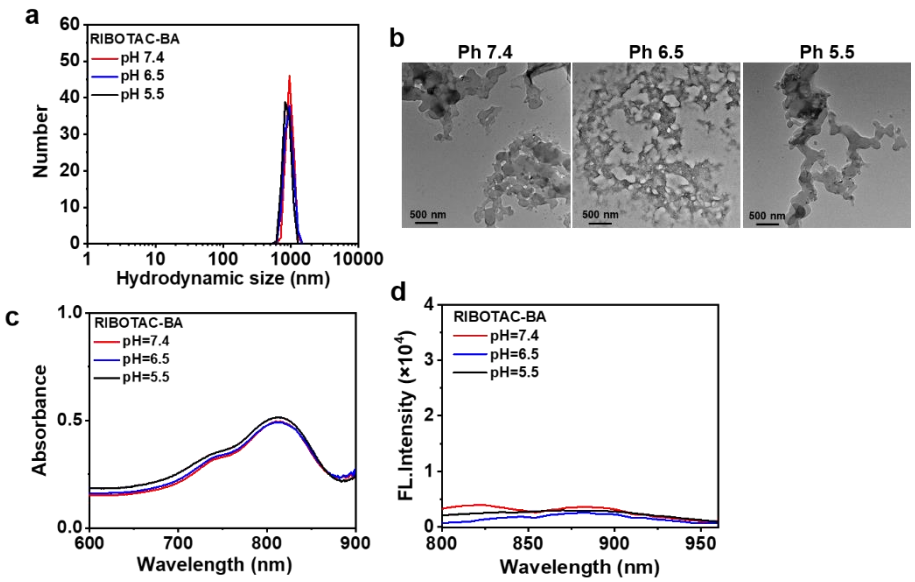

Supplementary Figure. 41. (a) DLS data, (b) TEM images (3 times the experiment was repeated with similar results), (c) Absorption and (d) fluorescence (FL) of RIBOTAC-BA in PBS buffer (pH = 7.4, 6.5, and 5.5). Source data are provided as a Source Data file.

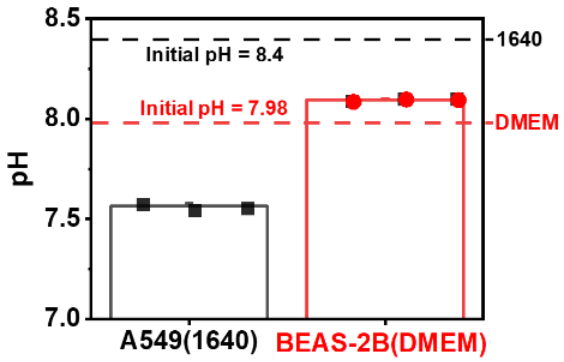

Supplementary Figure. 42. pH measurement of 1640 medium after 24 hours of A549 cells culture, and pH measurement of DMEM medium after 24 hours of BEAS-2B cells culture. The dashed lines represent the initial pH value of the medium. n = 3 independent samples, data denote the mean ± standard deviation. Source data are provided as a Source Data file.

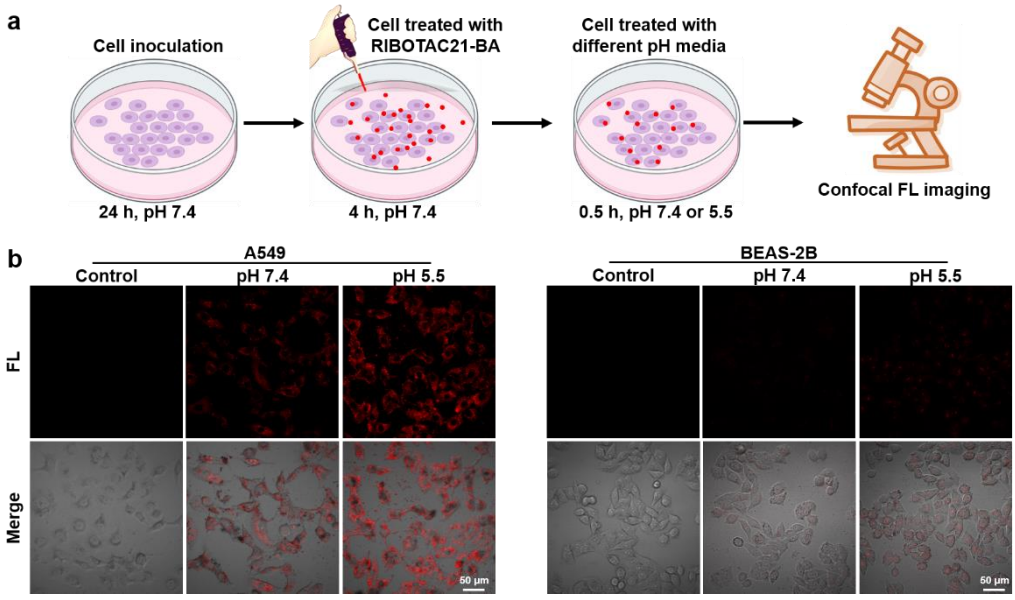

Supplementary Figure. 43. (a) Flow chart of RIBOTAC21-BA (5 μM) uptake experiment by tumor cells A549 and lung epithelial cells BEAS-2B. (b) A549 and BEAS-2B cells were cultured in medium containing RIBOTAC21-BA (5 μM) for 4 h, then the medium was sucked away and cultured in medium (pH =7.4 or 5.5) for 30 min, and then the fluorescence images of the cells were recorded by confocal. In the culture medium with pH=7.4, the fluorescence brightness of lung epithelial cells was significantly lower than that of tumor cells. In order to exclude the influence of the pH change of tumor cells on the fluorescence brightness, we further treated the cells with the culture medium with pH= 5.5, and the fluorescence brightness of tumor cells was still significantly higher than that of normal cells (scale bar = 50 μm). Supplementary Figure. 43a created in BioRender. Zhang, Y. (2025)

https://BioRender.com/s13n028.

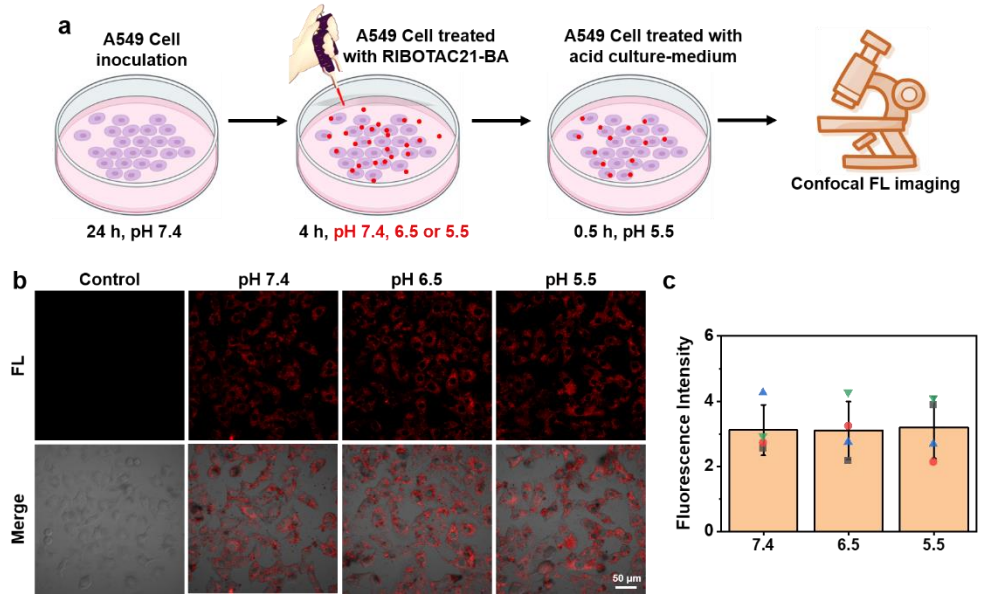

Supplementary Figure. 44. Uptake of RIBOTAC21-BA (5 μM) in A549 cells in the medium with different pH. (a) Experimental flow chart. (b) A549 cells were incubated with RIBOTAC21-BA in different pH medium for 4 h, and then replaced by fresh medium (pH = 5.5) for 30 min followed by fluorescence imaging. (c) Fluorescence quantification in Figure b. n = 4 independent samples, data denote the mean ± standard deviation. Source data are provided as a Source Data file. Supplementary Figure. 44a created in BioRender. Zhang, Y. (2025) https://BioRender.com/s13n028.

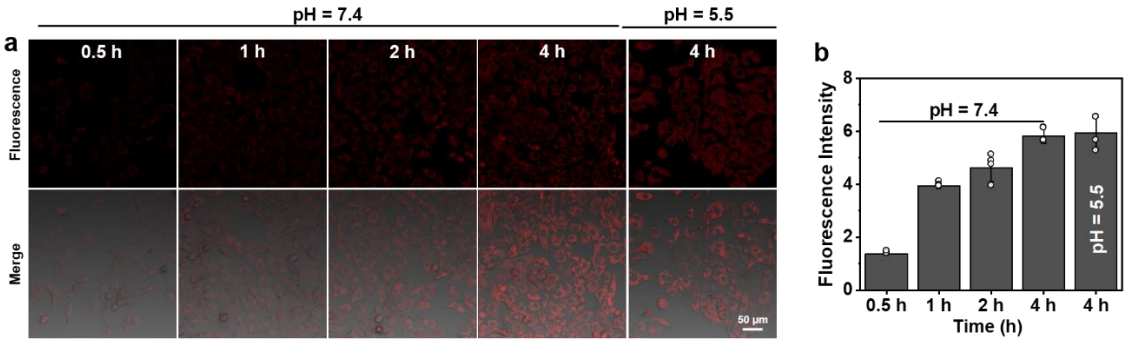

Supplementary Figure. 45. (a) Real-time FL images of A549 treated with RIBOTAC-BA (5 μM) in PBS buffer (pH = 7.4, 5.5). (b) FL intensity quantization of a (scale bar = 50 μm). n = 4 independent samples, data denote the mean ± standard deviation. Source data are provided as a Source Data file.

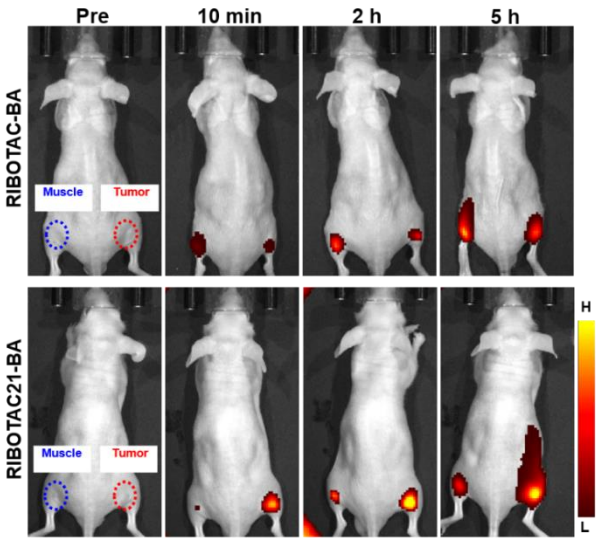

Supplementary Figure. 46. Real-time FL images of mouse treated with RIBOTAC21-BA and RIBOTAC-BA (16 μM, 50 μL) by intratumoral (right) and intramuscular (left).

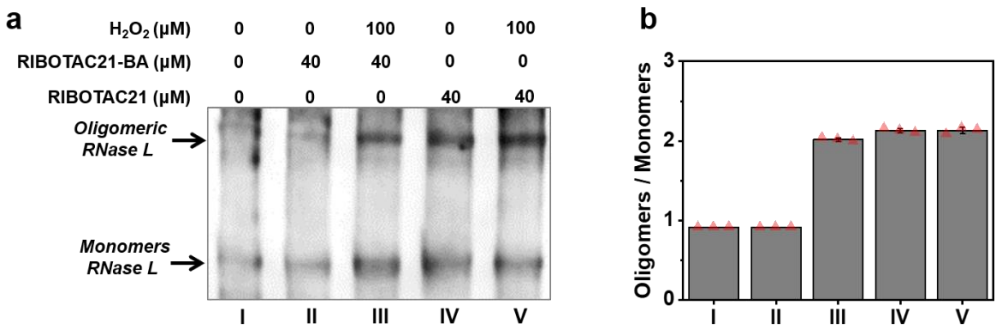

Supplementary Figure. 47. Representative PAGE gel images (a) and quantitative analysis (b) of the RNase L oligomerization induced by RIBOTAC21-BA+H_2O_2 or RIBOTAC21. n = 3 independent samples, data denote the mean ± standard deviation. Source data are provided as a Source Data file.

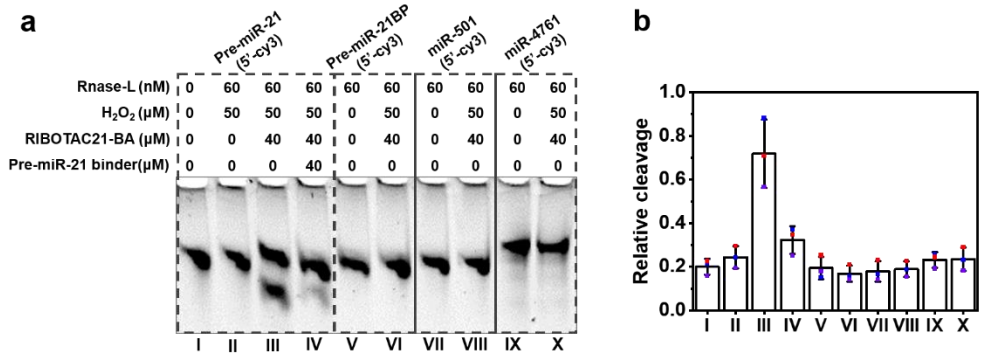

Supplementary Figure. 48. (a) Representative SDS-PAGE gel images of 5'-cy3 labeled RNAs (Pre-miR-21, Pre-miR-21BP, miR-501, and miR-4761) in aqueous solutions (pH=5.5) under different treatment conditions at 25°C for 12 h. Pre-miR-21 binder was compound **11**. (b) Quantification of miRNA degradation in a. n = 3 independent samples, data denote the mean ± standard deviation. Source data are provided as a Source Data file.

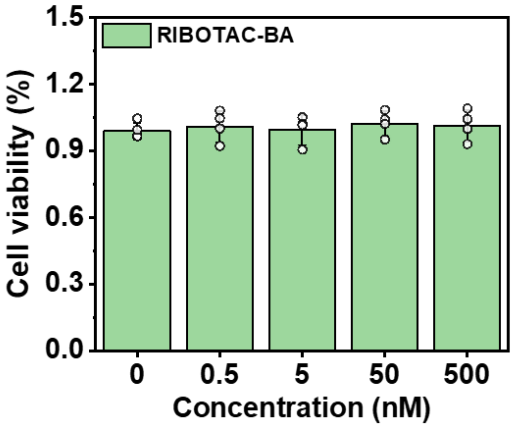

Supplementary Figure. 49. Cytotoxicity of RIBOTAC-BA to bronchial epithelial cells (BEAS-2B) detected by CCK8 assay. n = 4 independent samples, data denote the mean ± standard deviation. Source data are provided as a Source Data file.

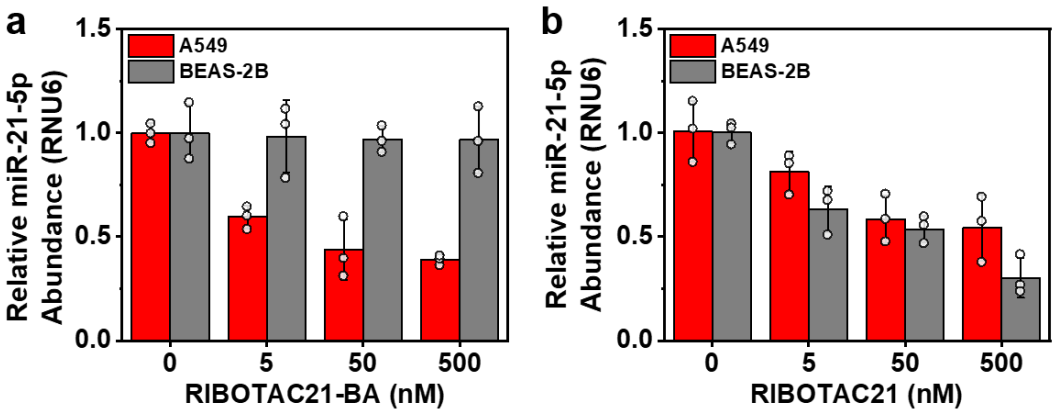

Supplementary Figure. 50. Effect of (a) RIBOTAC21-BA and (b) RIBOTAC21 on mature miR-21 levels in A549 and BEAS-2B cells at different concentration, as determined by RT-qPCR. n = 3 independent samples, data denote the mean ± standard deviation. Source data are provided as a Source Data file.

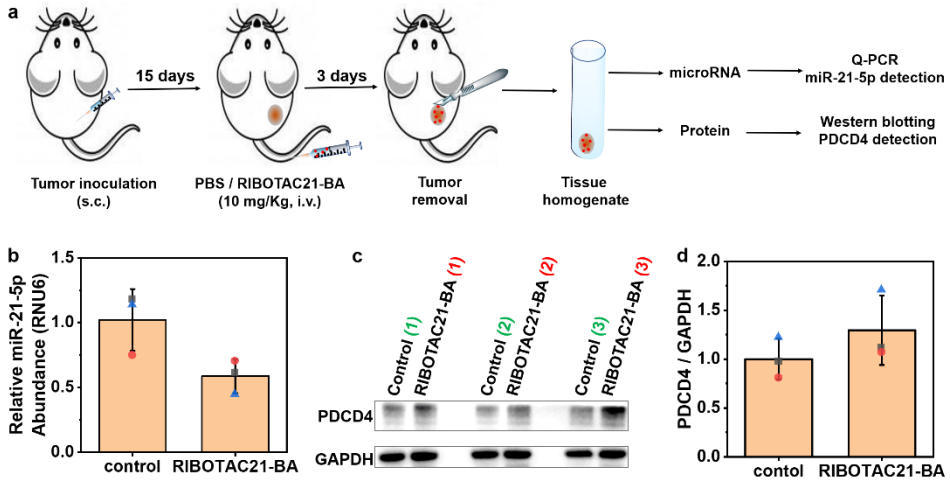

Supplementary Figure. 51. Effects of RIBOTAC21-BA (10 mg/kg, i.v.) on miR-21 and PDCD4 expression levels in A549 subcutaneous tumors-bearing mice. (a) Schematic diagram of the experimental procedure. (b) RT-qPCR analysis of the effect of RIBOTAC21-BA on mature miR-21 expression levels in A549 subcutaneous tumors. (c) Western blot analysis of the effect of RIBOTAC21-BA on PDCD4 levels in A549 subcutaneous tumors. (d) Quantification of PDCD4 protein levels as shown in (c). n = 3 independent samples, data denote the mean ± standard deviation. Source data are provided as a Source Data file. Supplementary Figure. 51a created in BioRender. Zhang, Y. (2025) https://BioRender.com/i42u241.

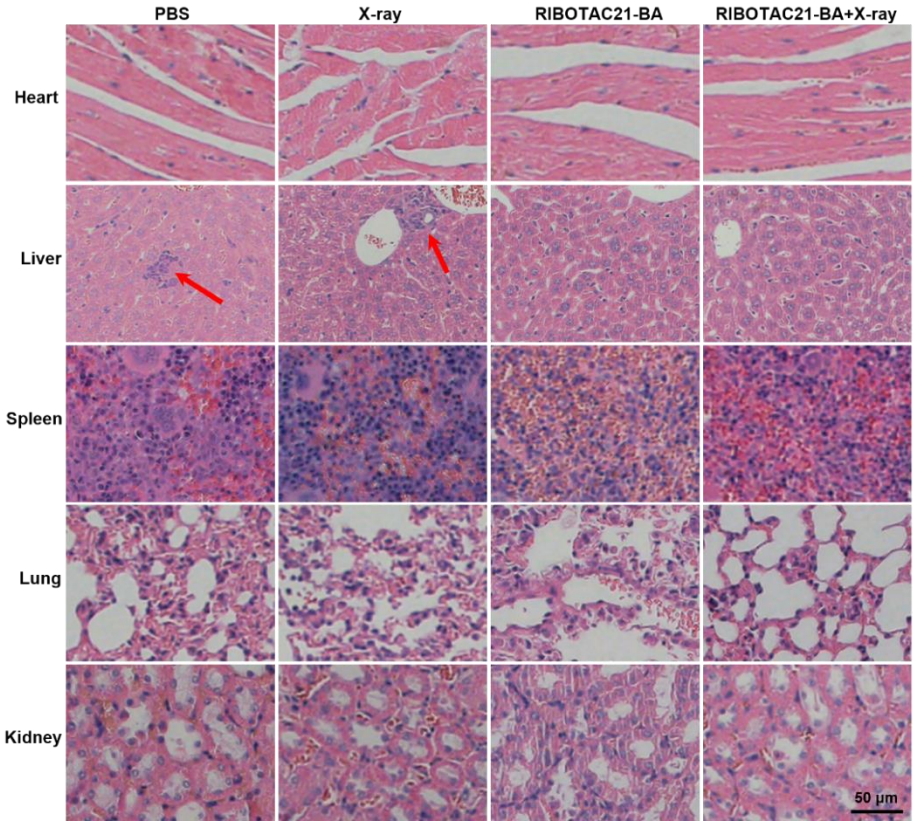

Supplementary Figure. 52. H&E staining of main organs from representative mice captured on 18 days after each treatment of Figure. 5 (n= 5 independent mice). Scale bar: 50 μm.

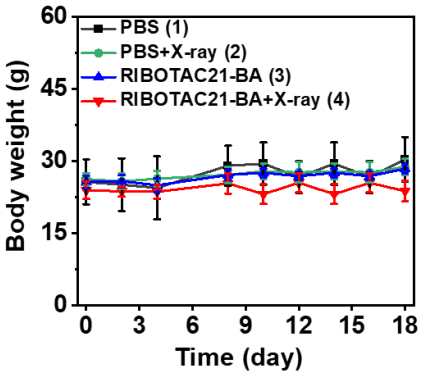

Supplementary Figure. 53. body weight variation of the mice after each treatment of Figure. 5 (n= 5 independent mice). Source data are provided as a Source Data file.

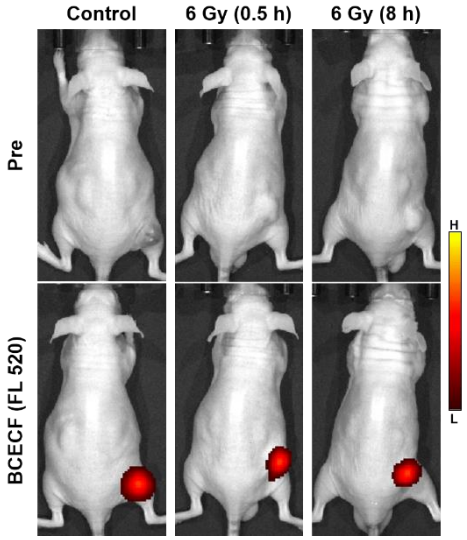

Supplementary Figure. 54. BCECF AM was used to monitor the pH change in tumors with or without X-ray irradiation (6 Gy). The pH detection reagent BCECF AM (5 μM, 50 μL) was injected into the tumors and fluorescence imaging was performed after 0.5 h (*Ex* = 480 nm, *Em* = 520 nm). No significant fluorescence change within tumors was determined, indicating that 6 Gy X-ray did not affect the pH value of the tumor microenvironment.

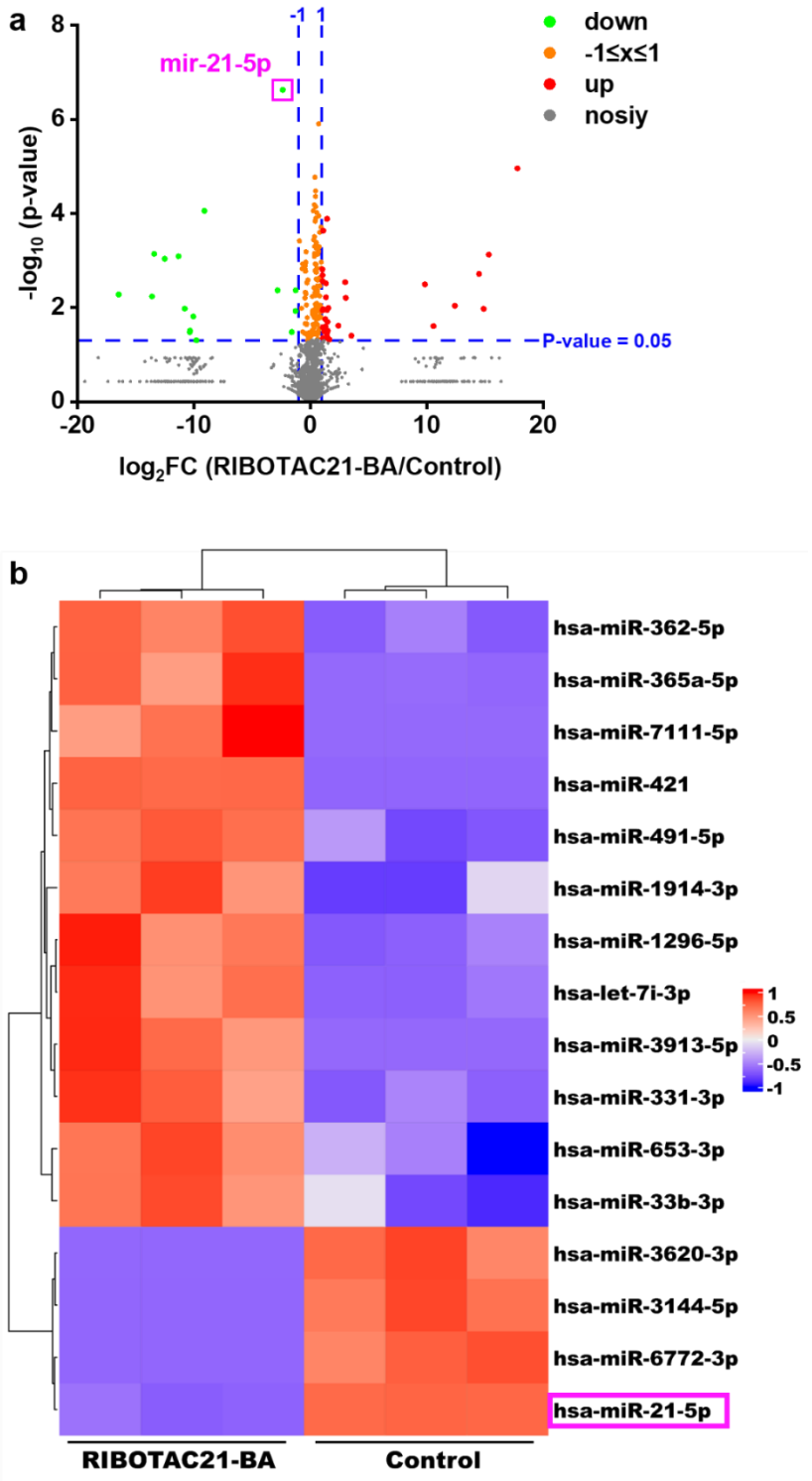

Supplementary Figure. 55. Small RNA sequencing analysis of A549 cells co-incubated with RIBOTAC21-BA (50 nM) for 48 hours. (a) Volcano plot of differential microRNAs. (b) Clustering heatmap of differential microRNAs. n = 3 independent samples. Source data are provided as a Source Data file.

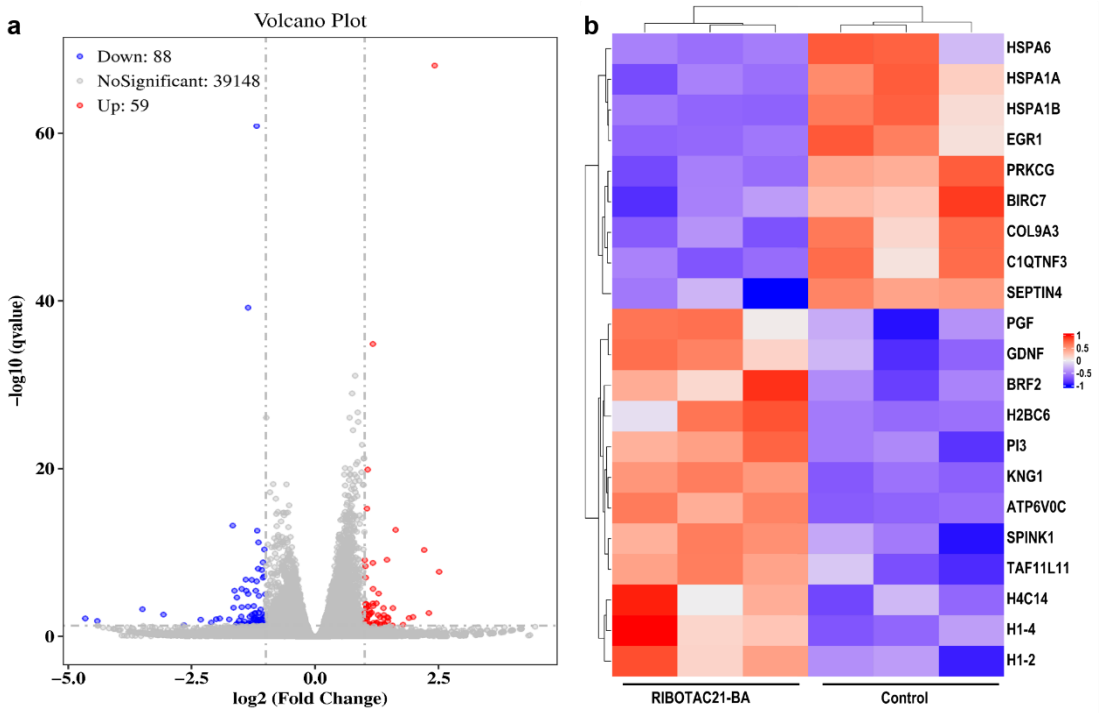

Supplementary Figure. 56. (a) Volcano plot and (b) Clustering heatmap of transcriptome analysis of A549 cells co-incubated with RIBOTAC21-BA (50 nM) for 48 hours. n = 3 independent samples. Source data are provided as a Source Data file.

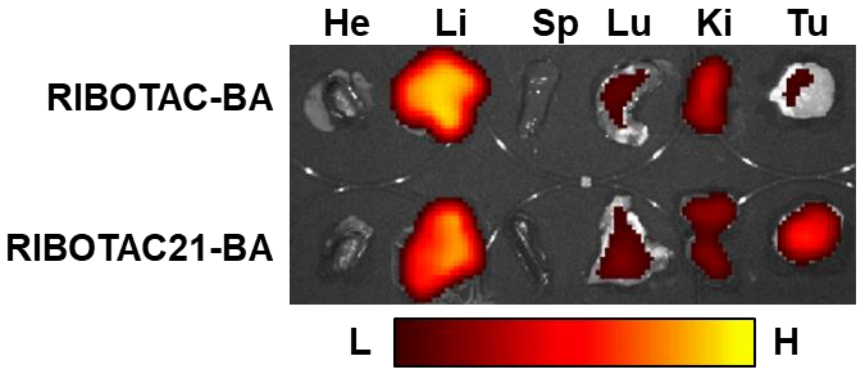

Supplementary Figure. 57. A larger version of the insert in Figure 3i.

Uncropped scans of gels in Supplementary Information file:

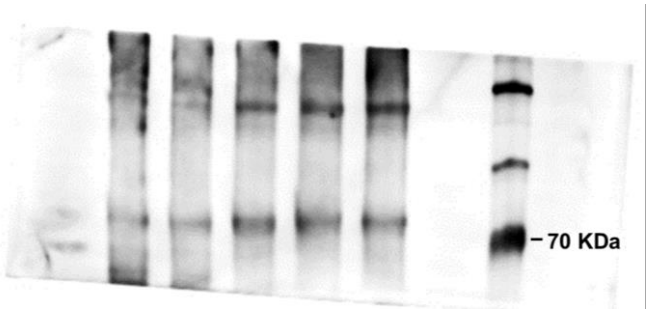

Supplementary Figure. 47a

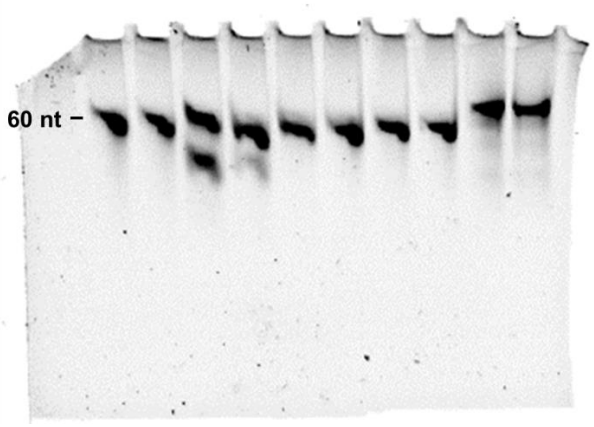

Supplementary Figure. 48a

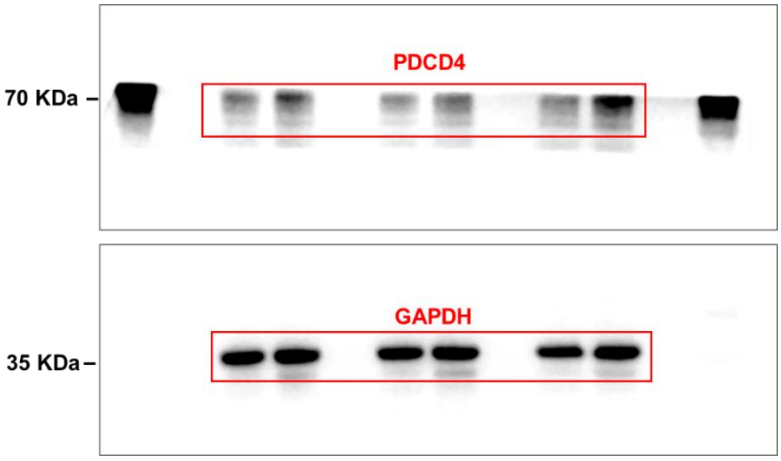

Supplementary Figure. 51b